SPECTROSCOPY AND MULTIVARIATE ANALYSES APPLICATIONS RELATED TO SOLID ROCKET NOZZLE BONDLINE

FINAL REPORT
CONTRACT NAS8-36955 D.O. 107
November 26, 1991

Prepared by
W. F. Arendale
Richard Hatcher
Brian Benson
Gary L. Workman

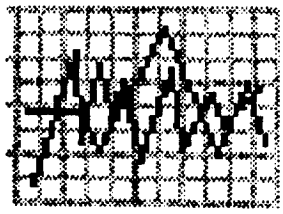

THE LABORATORY FOR INLINE PROCESS ANALYSES
THE UNIVERSITY OF ALABAMA IN HUNTSVILLE

(NASA-CR-184251) SPECTROSCOPY AND MULTIVARIATE ANALYSES APPLICATIONS RELATED TO SOLID ROCKET NOZZLE BUNDLINE Final Report (Alabama Univ.) ~~159~~ 58 p
CSCL 07D
N92-14134
Unclas
G3/25 0057119

SPECTROSCOPY AND MULTIVARIATE ANALYSES

APPLICATIONS RELATED TO SOLID ROCKET NOZZLE BOND

INTRODUCTION

The monitoring of manufacturing operations using combinations of optical fiber and spectroscopic techniques is an emerging technology. Optical fibers have many inherent advantages for applications related to quality assurance, nondestructive testing, NDT, and nondestructive evaluation, NDE. Unlike electrical conductors, optical fibers can transmit photons simultaneously in both directions. For example, a single fiber can both illuminate a test specimen and at the same time transmit back the optical signal resulting from reflection of photons. Individual fibers transmit data through intensity modulation, polarization modulation, or phase modulation of the transmitted light beam. A coordinated array of fibers is required for transmission of images. Fibers are electrically non-conductive. Since they are carriers of photons, they are neither a source of electromagnetic radiation nor are they affected by EMI or RFI. The bandwidth of low loss optical fibers is orders of magnitude larger than that of electrical conductors. Optical fibers are small and light weight. They are applicable in harsh environment. For examples, they can withstand relatively high temperatures and are not a source of ignition in combustible environments. They are compatible with structures made from composite materials. When fiber optics are embedded in composite structures, signals can be obtained which provide the information to monitor the performance of objects made from composites for chemical composition and mechanical properties including microstress and microstrain.

The availability of new and improved optical components has accelerated progress toward the development of photonic sensors using fiber optics. Photonic sensors, as transducers, are capable of detecting acoustic fields, linear and rotational acceleration, electric and magnetic fields, temperature, pressure, liquid level, chemical composition and many other parameters.

Chemical composition and molecular orientation define the properties of materials. Information related to chemical composition and molecular configuration is obtained by various

forms of spectroscopy. Chemicals that can be monitored during manufacturing processes include a large portion of all industrial chemicals as well as speciality products. Molecular weights range from high molecular weight polymers which are solids to low molecular weight gases. Quality assurance is improved when the analyses are immediately available. Just-in-time, real-time, and in-situ monitoring of chemicals requires that the operator have available in the plant many of the tools available to analytical chemists in the laboratory. In all situations, in-situ and on-site, techniques requiring minimal or no sample preparation are desirable.

The University of Alabama in Huntsville's Laboratory for Inline Process Analyses has demonstrated that a UV-VIS-NIR spectrophotometer which can be multiplexed to many sensors using fiber optic cables can satisfy all requirements for many applications. Technological improvements which have been made in fiber optic cables make it possible to connect a light source to a sensor by a fiber optic and observe the reactance of the sample through the same or a different fiber. A spectrophotometer and dedicated computer using low voltage rechargeable batteries can be portable for use anywhere in a plant or can accompany the field scientist.

Tests on a final product separate the acceptable from the non-acceptable product. The unacceptable product must be reworked adding the associated cost, or the unacceptable product is discarded with the cost added to the cost of the production of acceptable product. The challenge is to eliminate the manufacture of any unacceptable product and thus to eliminate the associated requirement to inspect the final product. This status can be achieved by providing real-time, in-process analyses. Production can be halted when an unacceptable product is recognized.

Software is responsible for conducting repetitive operations. Libraries of reactance signatures (reproducible images, spectra etc.) of compounds are stored in databases accessible to the computer. Software algorithms developed for multivariate analyses, expert systems, and Artificial Intelligence (AI) are used. The techniques are believed to be of particular significance toward achieving TQM objectives.

Science and engineering progress with the ability to measure. Today, new measurement techniques allow for the observation of smaller objects, observations at greater distances, and quantitation of smaller quantities, and more dilute samples. When these advances in instrumentation are combined with appropriate computer algorithms at each processing step the in-line and real-time process observations can prevent the manufacturing of unacceptable product.

OBJECTIVE

The objective for the experimental work described in this report was to obtain information related to the quality of the bondline in the solid rocket motor, SRM, nozzle. Hysol 934 NA, a room temperature curing epoxide resin, is used as the bonding agent. This material has a shelf life of 12 months and a pot life of 40 minutes. The adhesive is supplied in two parts which must be mixed in a 100:33 ratio. D.O. 107 under contract NAS8-36955 with Marshall Space Flight Center was to concentrate on measurement related to pot life. Correlations of this data with final bond properties were desired.

A good bond requires that the adhesive be placed on a properly prepared metal surface, that adhesive Parts A and B be mixed in appropriate ratio from material within shelf life specifications, and that the material be applied and the molded plastic insert be in place within 40 minutes after the adhesive is mixed. Spectroscopic data was obtained for surfaces prepared according to specifications, contaminated metal surfaces, samples of the epoxide adhesive at times that represent shelf aging from three months to two years, several mix ratio of A to B, and curing material. Temperature was found to be a significant factor. The study concentrated on pot life and mix ratio.

MODEL

Data is obtained through human observation without the aid of instruments and using instruments. Today, computers provide the digitized output from many transducers (mechanical and optical sensors). This raw data becomes useful information when it becomes related to the system being observed. A useful technique is to relate the data to a model. For many individuals, a model that simulates the process being monitored is the most useful. The

minimum requirement for a model is that it include the database of past experiences with a system and data currently being gathered to determine if the process is in the control region. The control region is defined by statisticians as a time domain where observations are normally distributed. The model should also predict the near future condition of the system and, most importantly, predict if the product is satisfactory for use in the next process or operation. Information taken at each point in the process should predict that inspection of the final product is unnecessary.

The pattern recognition approach as applied to in-process measurements can be stated as follows:

> Can we predict or infer properties of an object that we can not directly measure by using objects whose properties are already known and measurements that we can directly make on these objects? Additionally, do relationships exist in this measured data that are not obvious because they are hidden in a forest of numbers?
>
> Making a satisfactory product becomes a process of gathering objects available at each step in the process; making a wide variety of measurements on these objects; examining which measurements are useful; and developing prediction/classification models that permit the operator to infer values for the properties at the next step in the process and ultimately of the final product where the properties can not be measured.

A. STATISTICAL MODELS

Average, median, mode, geometrical mean, variance, standard deviation, standard error are useful statistical values. When these values for a variable are plotted on control charts, the concepts of upper control limit, UCL, and lower control limit, LCL, frequently plus or minus three standard deviations, suggest when a process is "out of control". At the control limits corrective action for a process or rejection for a raw material or a product is necessary.

It has been demonstrated that extremely small quantities of chemicals can contaminate a surface making bonding to the surface difficult. Dilute quantities of a foreign substance in a resin mixture may affect the physical properties or the kinetics of a reaction. As the desire to improve product and eliminate unacceptable product increases, the requirement to investigate new techniques that extend the level of detection to smaller quantities and more dilute solutions is ever present. Some results from The Laboratory of Inline Process Analyses at The University of Alabama in Huntsville are described in this report. Narrower control limits are possible through the use of multivariate statistics and fiber optic spectroscopy.

B. MULTIVARIATE STATISTICS

Spectrophometric methods with a two standard deviation of 10 percent are accepted. A smaller standard deviation requires careful control of analyte concentration and particles in the solution that scatter light. The random number generator in the Statgraphics software package was used to generate a series of random numbers having the following properties:

Sample size	100
Average	10.0143
Median	9.9763
Mode	9.9696
Geometric Mean	10.0083
Variance	0.1212
Standard Deviation	0.3481
Standard Error	0.0348
Minimum	9.3136
Maximum	10.8843
Range	1.5707

The 100 values are plotted in Figure 1. The 100 values were generated as 5 sets of random numbers having mean values of 9.50, 9.75, 10.00, 10.25, and 10.50 with a standard deviation of 0.25. The five sets are shown in Figure 2 as 5 barrels filled with the five sets of data. The numbers could represent the values obtained from an analytical procedure with a 2 standard deviation of 5 percent. The production streams, assuming that the drums were filled in other orders, are shown in Figure 3. Each of the production streams would have the same descriptive statistics if the entire production was dumped into a tank and 100 analyses were

made on samples taken from a well blended tank using a procedure with a 2 standard deviation of 7 percent. The material when blended in the tank is within production specifications as determined by the analytical procedure. The deficiencies in sampling blended material are driving forces for the search for on-line real-time analyses. If a spectrophotometric sensor with the same precision as the analytical method were mounted in the pipe, the values would represent instantaneous digital readings. Achievement of in-line real-time analyses eliminates the delay in obtaining information required when it is necessary to take a sample and carry it to a laboratory for analyses. Information from in-line real-time analyses can also be immediately used in control loops to take corrective action or to stop a process.

The use of random numbers to represent analytical values requires additional considerations. The failure to recognize variance in all measurements including analytical results can result in undesirable outcomes. The sources of variance in data are often disguised. The numbers in the examples would be expected if a 12 to 16 bit high frequency analog to digital converter was used to digitize the electrical voltage from a transducer. Production monitors are frequently analog gauges. The needle on the gauge moves about a central position. The amount of movement depends on the mass of the needle, the power of the amplifier driving the needle, and the resistance-capacitance network used to integrate instantaneous values. Driven by the human mind, the eye is usually an excellent integrator for determining the central position of the needle or recognizing the equipment is malfunctioning. Duplicating these human characteristics in a computer driven measuring system is not a trivial matter. When a computer program initiates a sampling event, a digital value is produced. No information is recorded concerning fluctuations about this value. In addition, the new database contains no information

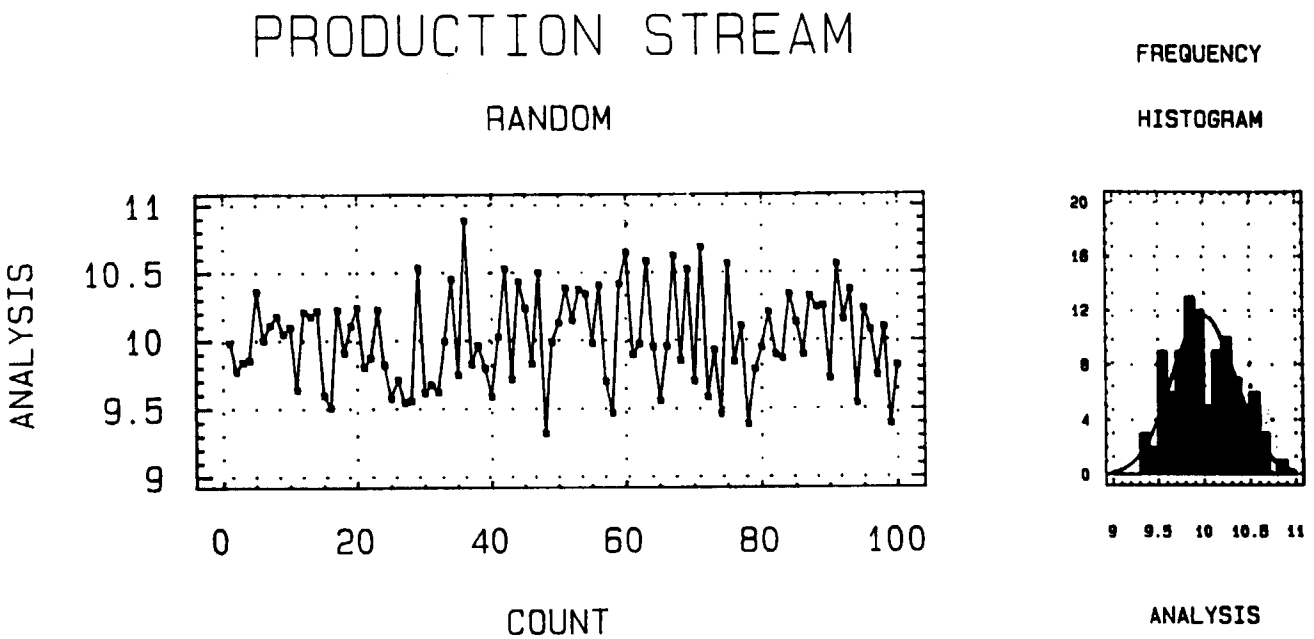

Figure 1. Production Stream Random Numbers

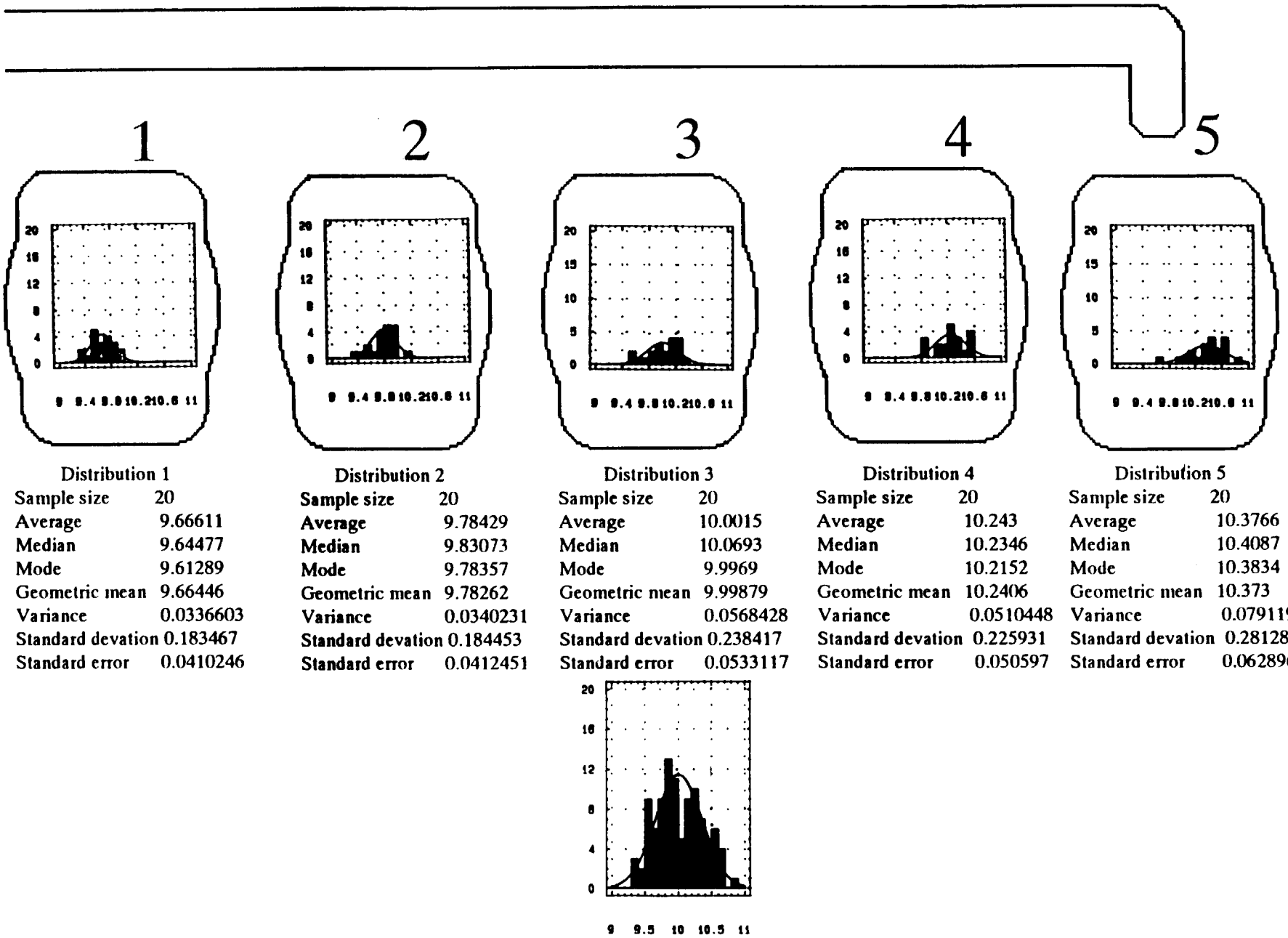

Distribution 1	
Sample size	20
Average	9.66611
Median	9.64477
Mode	9.61289
Geometric mean	9.66446
Variance	0.0336603
Standard devation	0.183467
Standard error	0.0410246

Distribution 2	
Sample size	20
Average	9.78429
Median	9.83073
Mode	9.78357
Geometric mean	9.78262
Variance	0.0340231
Standard devation	0.184453
Standard error	0.0412451

Distribution 3	
Sample size	20
Average	10.0015
Median	10.0693
Mode	9.9969
Geometric mean	9.99879
Variance	0.0568428
Standard devation	0.238417
Standard error	0.0533117

Distribution 4	
Sample size	20
Average	10.243
Median	10.2346
Mode	10.2152
Geometric mean	10.2406
Variance	0.0510448
Standard devation	0.225931
Standard error	0.050597

Distribution 5	
Sample size	20
Average	10.3766
Median	10.4087
Mode	10.3834
Geometric mean	10.373
Variance	0.0791193
Standard devation	0.281282
Standard error	0.0628965

Figure 2. Random Numbers - Size 20

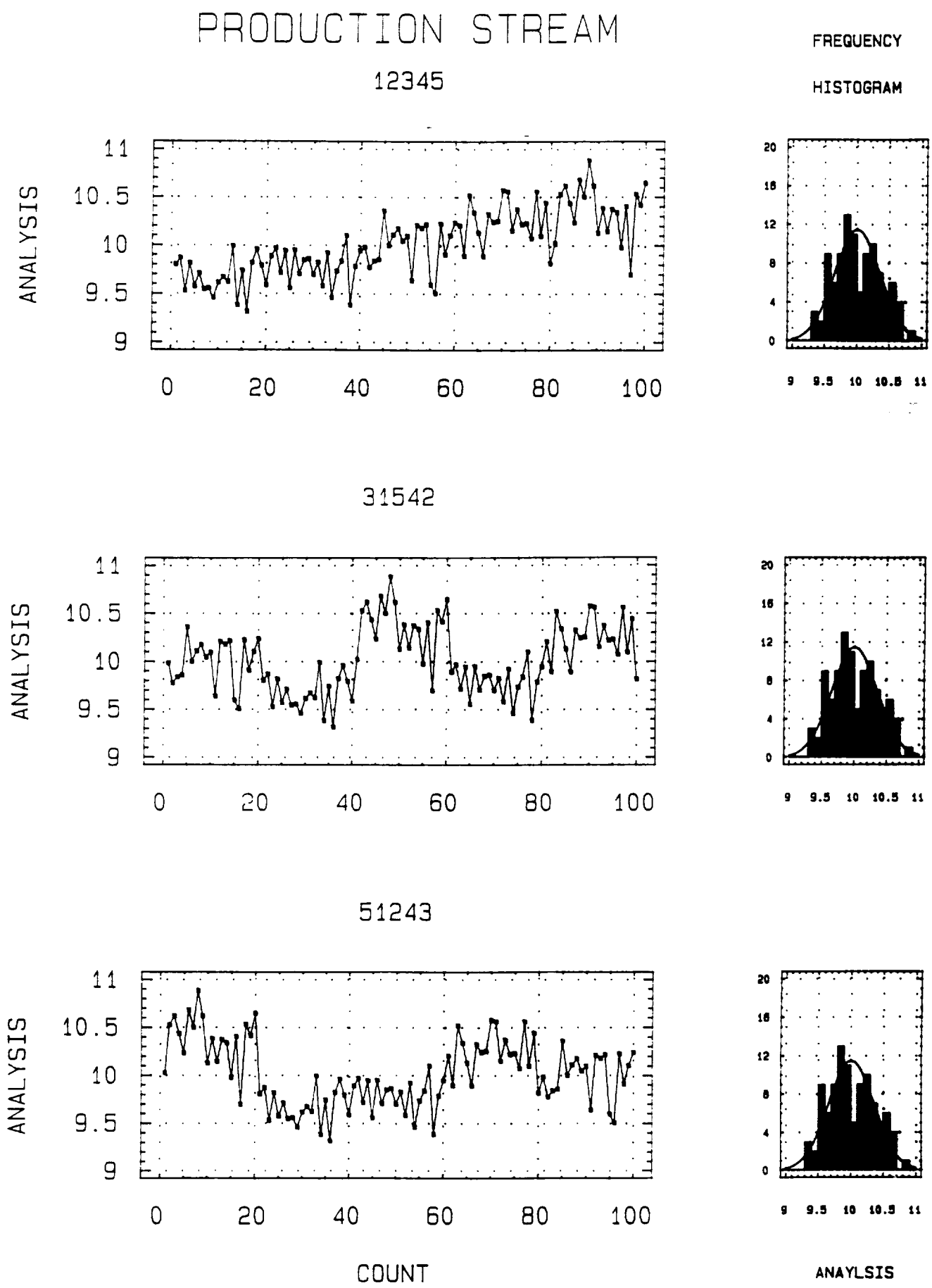

Figure 3. Production Stream - Reordered

as to what happened between the recorded digital values. The programmer can attempt to emulate the human mind by requiring many values to be taken and using the average. If the noise, non-sample information, is Gaussian a large number of values will average to the central value. Time is consumed when taking the average of multiple readings. If a moving stream is being observed, if a chemical reaction is continuing, or if large surfaces are being scanned, the loss of information caused by less frequent sampling can be important. If the transducer is in a well blended composition and time is not important, then the noise can be integrated out. However, if the detection limit is of the same magnitude as the noise variance, information concerning the analyte will be limited. When plotting control charts one compromise is to use time weighted or running averages. These methods can be very effective when treating analog values and decisions are made on trends rather than individual values. These concepts are very difficult for the computer programmer to emulate.

When values are randomly distributed, no corrective action should be taken. This axiom is especially true when viewing real-time values. In practice in-line analysis values often show greater variance than the values for samples from a well stirred tank because composition does vary with time. If TQM requires greater knowledge concerning the process, what are the alternatives? The best option is usually to make measurements upstream from this measurement point. If the process is a batch process that is being dumped through the pipe, place the sensors in the process container. Increase yields have been obtained by following a reaction in this manner.

Chemometrics is an interdisciplinary activity that includes computer science, statistics, and chemistry. Within a university administrative structure, practitioners will often be located in the analytical chemistry unit. An objective of chemometricians is to capture as much reliable information as is obtainable from a data set. Often data from a sensor is obtained at low signal to noise ratio and smoothing of a data vector is a necessity. A spectrophotometer with a dedicated computer increases the number of options available to the chemometrician. The spectrophotometer can take measurements at multiple wave lengths and provide multidimensional data. One algebraic equation can be solved for one unknown. Two

independent equations are required to solve for two unknowns. In theory a set of multiple wavelength spectra could be used to quantitate as many analytes as there are data points. A major advantage of spectra, data points taken at multiple wavelengths, is that nonaborption at a wavelength can provide knowledge of the same magnitude as an absorbing wavelength that follows Beer's Law. No two molecules have identical spectrophotometric signatures, spectrum.

Multivariate analyses and/or analyses of variance methods have been recognized and used for many years. The popular software product SPSS (Statistical Programs for the social sciences) is now in the eleventh version. Nearly all of the algorithms used in the applications software available for multivariate statistical evaluations of data, directly or indirectly, use the variance-covariance matrix. Therefore the programs are searching for variance. The search techniques are supported by sound mathematical and statistical theory. The techniques isolate abstract factors. The identification of meaning of these abstract factors in the real world is the responsibility of the user. Methods have been described for rotating the abstract orthogonal vectors so that the investigator has a better chance of recognizing the sources of variance. This remains a difficult problem in the social sciences. First, a person being observed is often affected by the presence of the observer. Second, the number of samples in a population is often small. When these procedures are used to discover sources of variance in the physical sciences, neither of these problems exist. The experimenter can change the experimental conditions, but the presence of the experimenter is not believed to change the response of the molecules. The predominant theory in the physical sciences, rlated to physical change, is the Kinetic Molecular Theory. A hypothesis of this theory is that molecules can be described as statistical populations. Also a mole of molecules contains 10^{23} molecules. Chemical systems should conform to the assumptions of the statistical procedures.

When working with small quantities and low concentrations that push the limits of detection, the information is embedded in signals characterized by low signal-to-noise ratio. This often leads to lack of understanding and difficulties in communicating with individuals who hold to the tradition that a measurement can be made to an absolute standard. Many scientist and engineers have not been introduced to the techniques of multivariate analyses as provided to

analytical chemist by Wold, Kawolski, Malinoiski, Massart, Martens, and their many associates (1).

It is the practice at The University of Alabama in Huntsville Laboratory for Inline Analyses to record absorption values at as many wavelengths as the memory capacity of the computer will allow and to average only a small number of values for each wavelength. Principal component analysis is used to obtain qualitative and quantitative information. The concept of principal component analysis is shown in Figure 4.

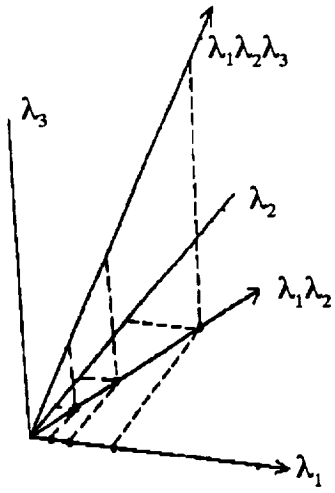

Figure 4. Representation of principal component analyses.

If three samples of a pure material at three concentration levels were being considered, the absorptivity values for the three concentrations at λ_1 could be plotted on the λ_1 axis. In a similar manner the absorptivities for the three samples at λ_2 could be plotted on the λ_2 axis. Both the values on the λ_1 and the λ_2 axis could be projected on the λ_1 λ_2 axis. If there was no noise in the measured values then the projections would coincide. This process could be continued for as many wavelengths as desired. The axis that is the best representation of all of the data is the principal component axis. Evaluation of a data matrix represents the reverse process. The axis that removes the greatest variance is calculated. The first component is

subtracted from the variance-covariance matrix and the search repeated. We then have the second component. The processes of subtraction and search are repeated until the vectors represent noise. Two questions must be answered. How many of the components are real components and what are the spectrum of the real components. Many procedures have been proposed to answer the first question. A Scree plot is frequently used. Each component represents less and less of the variance. When the sum of the variance become large and little improvement is gained by adding another component, a good compromise has been reached.

The question of what the principal component represent is more difficult. Target factor analysis represents one method (2). If the analyst expects that a component is present and has the spectrum of that component, this spectrum can be multiplied into a variance - covariance matrix to find the rotation required to yield this spectrum. It is possible to use this method to construct a rotation matrix and identify; the concentration of each component. This procedure requires the K Matrix, the extinction coefficient spectrum for each component in the mixture. Frequently the spectrum of some of the components in a mixture are not available and other methods must be used.

Unless the analyst wishes to establish a relationship with an interpretation based on causality, it is not necessary to identify the component or factors to perform quantitative analyses for known components. To use this method a calibration set is required to meet the following conditions.

1. Typical samples are available for the training set.
2. The samples span each of the individual phenomena that can be controlled.
3. The samples are randomly selected to insure a chance of spanning the noncontrollable phenomena.

DESCRIPTION OF THE GUIDED WAVE SPECTROPHOTOMETERS

The Laboratory for Inline Process Analyses uses the spectrophotometers manufactured by Guided Wave, Inc. Guided Wave, Inc was founded by Mr. David LeFebre in May 1983 to manufacture research grade spectrophotometers. Mr. LeFebre's immediate past experience had been in research and manufacturing of optical fibers. Developments have concentrated on using single-strand fibers to connect the spectrophotometer to the sensor. In early spring 1984, UAH purchased one of the first five of the Model 100 instruments manufactured. The Model 100 was the first spectrophotomer to optimize the optical components to the characteristics of energy transmission over fibers. All feedback from users has been taken seriously and used in developing new models. The Model 300 double beam instrument, on the market for about one year, was an attempt to include the needs of all users. The original instrument purchased by UAH has been updated on three occasions as the Model 150, Model 200, and Model 260 were developed.

Some features of the Guided Wave instruments are described in the following sections to illustrate the requirements on an instrument which is to be used with single-strand fiber optics and to provide examples of the apparatus used to obtain the experimental data.

A. THE OPTICAL BENCH

The design of classical spectrophotometers includes slits, mirrors, gratings or prisms to disperse the radiation, and a detector. There is a loss of energy at the surface of each component. Since the energy carried by a fiber is small, as many surfaces as possible are eliminated. The essential elements of the fiber spectrophotometer are shown in Figure 5.

The light source is a tungsten halogen bulb or a deuterium lamp. The light source is large with respect to the diameter of the fiber core. Lens are used to focus the energy from the source onto the fiber.

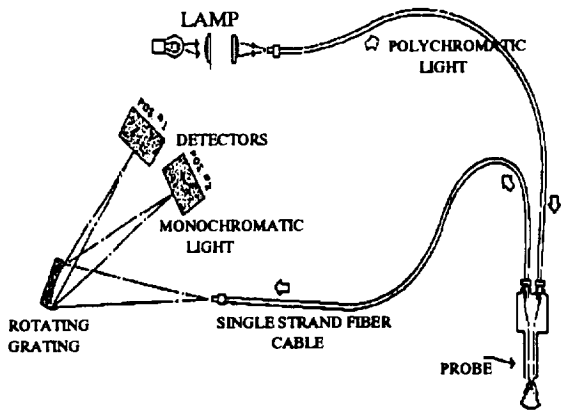

Figure 5. Scanning Fiber Spectrophotometer

The entrance cone into the fiber is controlled by the numerical aperture of the fiber. The fiber transmits the energy to the sample. Shown in Figure 5 is a transmission probe where the energy from the exit cone of the fiber is focused onto a concave mirror. The mirror focuses the energy back onto a second fiber that carries the energy to the spectrophotometer. The cone of energy from the fiber falls on a holographic concave diffraction grating. Since this cone is fixed by the characteristics of the fiber, the size of the grating that can be filled with light is determined by the distance from the end of the fiber to the grating. To reduce stray light in the grating chamber, a square aperture is used so that the cone of light just fills the square grating. This is the only point at which slits are used in this spectrophotometer. The longer the distance from the aperture to the grating, the larger the area of light available but the lower the intensity. The Guided Wave instruments are 0.25-meter spectrophotometers. A characteristic of holographic concave gratings is that the reflected energy can be focused to a spot for only two wavelengths. The grating in this spectrophotometer has been designed so that the distance between these spots is sufficient that two detectors can be mounted on the instrument at the same time. The software can be set to change between the two detectors at any selected wavelength. The pattern of the radiation is shown in Figure 6.

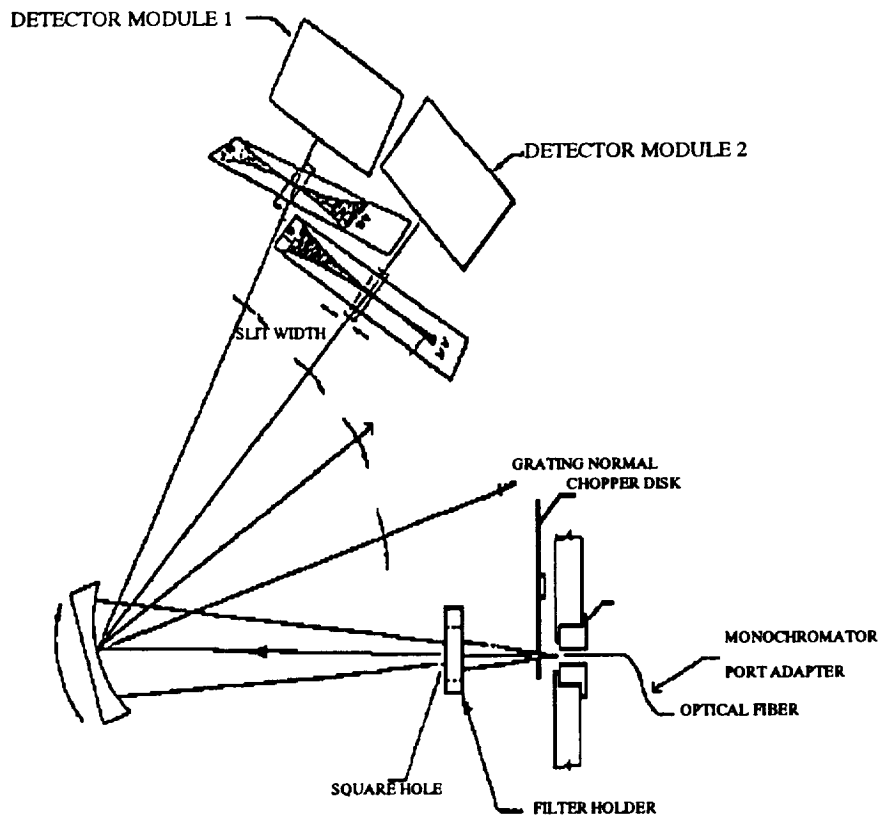

Figure 6. Radiation Pattern at the Detector Slits

B. GRATINGS AND DETECTORS

Changing a grating or detector only takes a few minutes. Therefore, observations can be made from the ultraviolet to the near infrared with the same instrument by choice of gratings and detectors. When quartz fibers are used, the useful region is from 200 - 250 nanometers to 2.2 micrometers. Zirconium fluoride fibers are available to extend the observation region to 3.2 micrometers in the infrared. To cover the full range at high resolution photomultipliers, silicon, germanium, and lead sulfide detectors are required. To cover the entire range diffraction gratings at 1200, 800, 600, 300 lines/mm are used. A component selection guide from the Guided Wave, Inc. literature is shown as Figure 7.

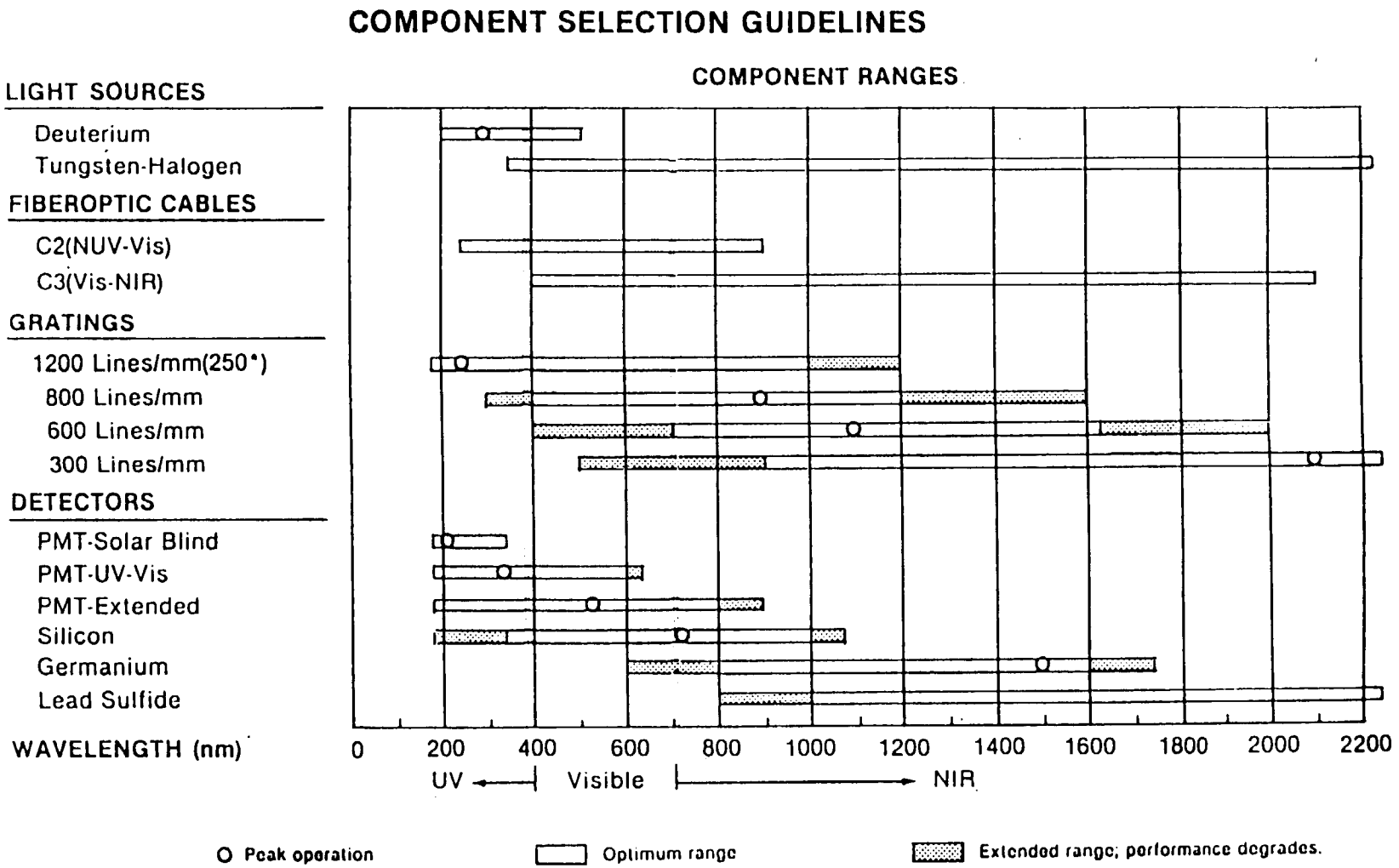

Figure 7. Diffractions Gratings and Detectors

C. EXPERIMENTAL SETUP AND PROBES

The spectrophotometer is remote from the sample as the spectrophotometer is connected to the sample by a flexible fiber optic cable and the sample is connected to the spectrophotometer by a second fiber optic cable. This provides flexibility equal to the imagination of the experimenter. Standard probes and components as shown in Figure 8 are used to gain experience with the concepts. As the real-time problem is defined specialized components are designed to interface the system with the fibers that carry the information.

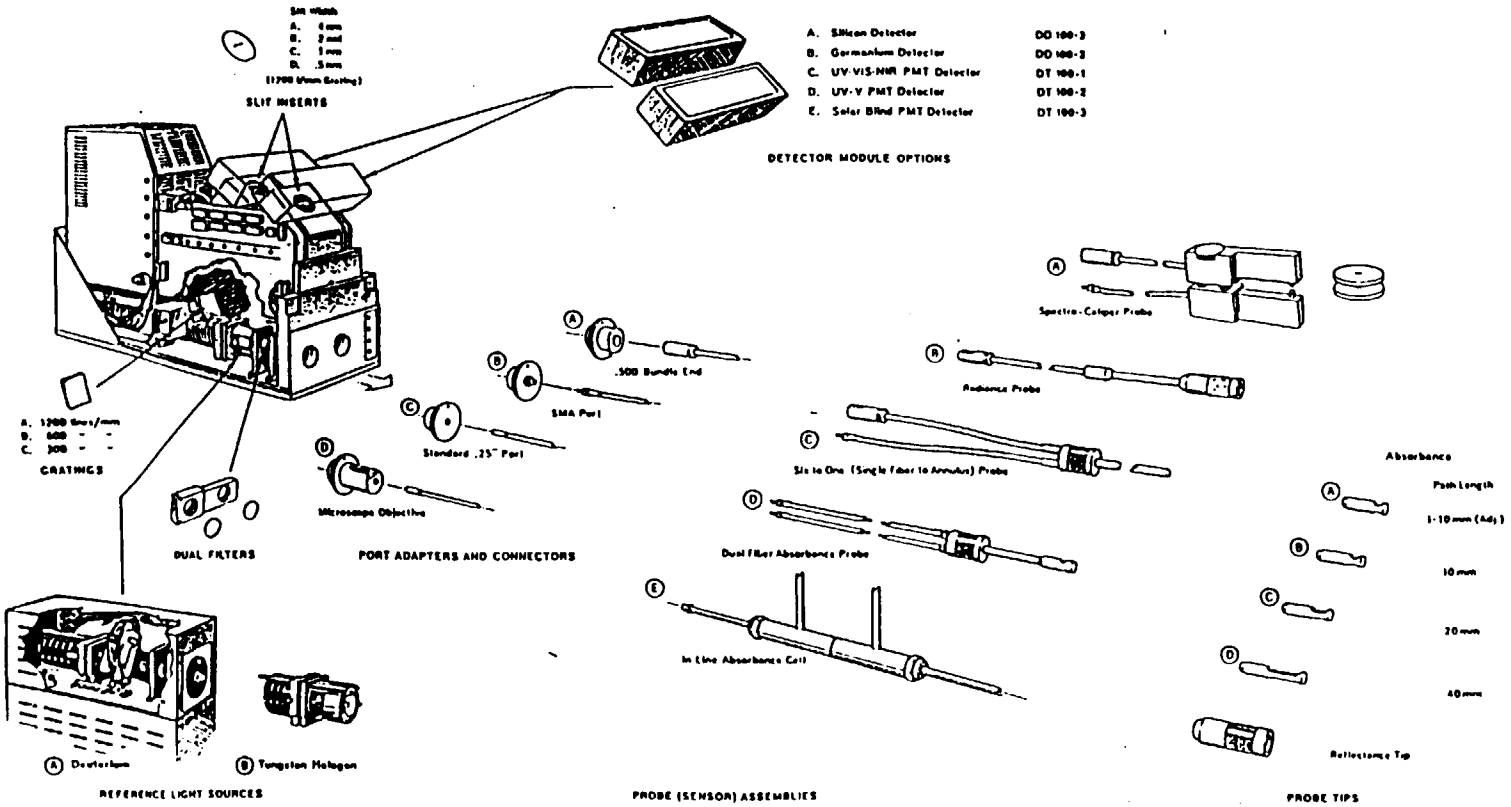

Figure 8. Systems Components

REFLECTION SPECTROPHOTOMETRY

A. APPLICABLE OPTICS THEORY

Arendale and Jeffreys (3) at the University of Alabama in Huntsville Research Institute in 1967 conducted an experimental study related to reflected energy from laser illuminated targets under U.S. Army Grant DA-ARO-D-31-124-12761. The University of Alabama in Huntsville was one of the first institutions to become active in the study of remote spectroscopy and spectroradiometry.

Measurement of the characteristics of scattered radiation can provide significant information about a surface.

1. Reflection of Radiation From a Nonabsorbing Surface

The first consideration in the study of reflected energy from a particular surface must be an evaluation of the general reflection characteristics. Most texts on illumination engineering recognize two extremes of reflected energy, specular represented by (A) and Lambertian represented by (B) in Figure 9. If a surface is polished (microscopically smooth) it reflects; that is, the angle between the reflected ray and the normal to the surface will equal the angle between the incident ray and the normal. A perfectly reflecting surface, will reflect all of the energy with the same angular dispersion as the incident beam. If a material has a rough surface or is composed of minute crystals or pigmented particles, the reflection is diffuse. Individual rays obey the laws of specular reflection; but, since the surface is rough or the particles may be in different planes or different orientations, the light is reflected in all possible directions. A Lambertian surface is defined as a surface where the intensity of reflected energy is independent of the angle of observation. Lambert's Law (based on many observations and not theory) can be stated:

$$I_r = I_o \cos\theta \cos\psi$$

where I_o is the intensity of the radiation at normal incidence, θ is the angle of incidence, and ψ is the angle of observation. Many combinations of specular and diffuse radiation are observed from real surfaces. Four frequently observed patterns are shown in Figure 9. as C, D, E, and F. Much work has been done, particularly by illumination engineers to describe the intensity of radiation from a surface under various lighting conditions. Also, many references can be found to studies of polarization upon specular reflection. Fresnel's formulas for the reflection of polarized radiation can be found in most textbooks on optics.

2. Effect of an Absorbing Film on a Reflecting Surface

When the reflecting surface absorbs radiation at a given frequency, or if an absorbing thin film covers the surface, the chemical composition can often be identified. The use of polarized monochromatic radiation (obtained from monochromators) to measure the index of refraction and the absorption coefficient of thin films is an important scientific tool. Chemical analyses by spectroradiometry and reflection spectrophotometry have become important tools available to the material scientist. The use of monochromatic polarized radiation is often referred to as external reflection spectroscopy. The use of parallel polarized light requires specialized equipment . No work has been included in this D.O.

3. Absorption by Transparent Substances

When monochromatic light passes through an absorbing medium with the incident beam collimated and normal to the surface, the intensity of the ray decreases exponentially. This phenomena frequently follows the Beer - Lambert Law:

$$A = \text{Log } I/I_o = E\,C\,L$$

where A is the absorptivity, I is the intensity of light passing through the sample, I_o is the original intensity, E is the absorptivity coefficient, C is the concentration expressed in moles/liter, and L is the path length.

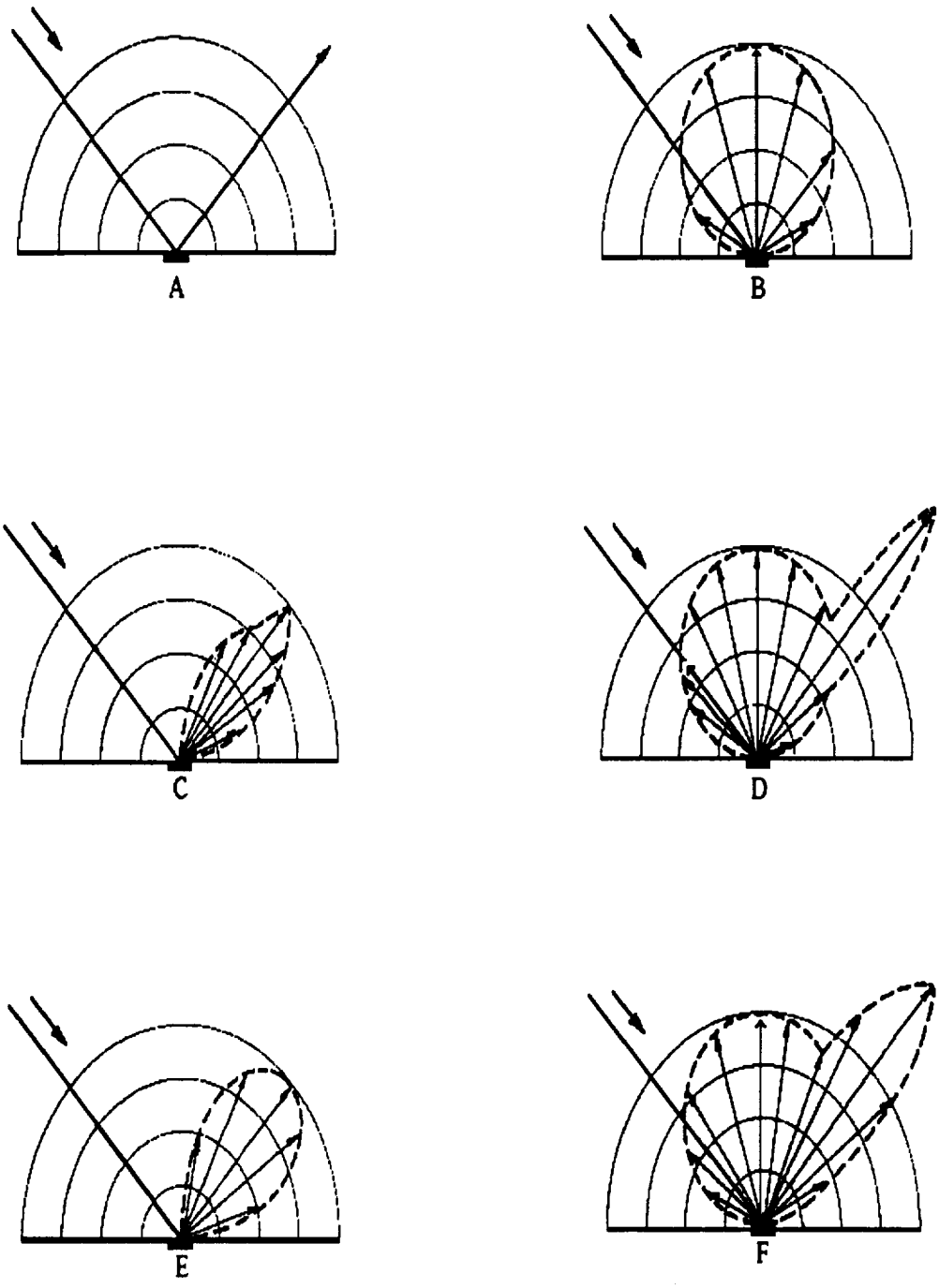

Figure 9. Patterns For Reflected Light Rays

The Beer-Lambert Law must be modified for reflection spectroscopy. A rough surface scatters radiation. If the surface is Lambertian, it is scattered equally in all directions. If there are surface imperfections greater in size then the wavelength of the observing radiation there will be specular scattering. The radiation patterns have been described using Figure 3. If superimposed on the scattered radiation patterns is an absorption due to a contaminant, the two effects combine to give a measured intensity less than the illuminating beam. Identification of the contaminant requires a multiwavelength spectrum. For practical analytical purposes the reflectance spectra are generally analyzed by using one of the so-called two parameter theories. A comparison of the Kubelka-Monk, Rozenburg, and Pitts-Giovanelli methods has been made by Hecht (4). The Kubelka-Monk algorithm is found in many software packages used by analytical chemists. The solution for a thick semi-infinite scattering layer can be written in the form:

$$f(R) = \frac{(1 - R)^2}{2R} = \frac{K}{S}$$

where R is the measured reflectance, and K and S are the absorption and scattering coefficients. Application of this equation is made assuming the absorption constant, K, to be the product of the concentration of the absorber and the appropriate absorptivity. The scattering characteristics on the other hand are often determined by a carrier material of nearly constant composition, analogous to the solvent of transmission spectroscopy. If S is constant the equation becomes and

$$f(R) = \frac{E}{S} = kC$$

only one parameter k must be determined for quantitative analyses. It is this simplicity that is believed responsible for the wide-spread use of the Kubelka-Monk theory, despite the fact that it has been shown to apply quantitatively in many cases over only a limited range of concentrations. In addition to the Kubelka-Monk theory many other functions have been used successfully for NIR spectroscopy. Frequently log(1/R) has been used successfully. The range of concentrations investigated is usually small. This probably accounts for the success of the several formulas that are found in the literature. We investigated the absorption of eosin on thin

layer chromatography plates and found the Kubelka-Monk theory applicable over 7 decades of concentration. Therefore, we use the Kubelka-Monk formula for many of our experiments.

B. INSPECTION OF ROUGH METAL SURFACES

An important criteria for obtaining proper adhesive bonds between metal and plastic parts is a clean metal surface. The surfaces frequently are machined, cleaned with air blasts containing abrasives, and then cleaned with solvents. The surfaces are rough and give near Lambertian patterns of diffuse reflection. Diffuse reflections are wavelength dependent. If the surface is illuminated with radiation from a white light source and the resulting spectra displayed as observation angle vs intensity of reflected energy at multi-wavelengths, a clean uniform surface should give a signature with the values normally distributed. When a contaminant covers a portion of the surface, absorptions at wavelengths characteristic of the contaminant will be observed.

For the experiments described in this report a 5 x 5 x 5 centimeter aluminum block supplied by Marshall Space Flight Center was used. Since this D.O. was for a survey of capabilities of reflection spectroscopy, no minimum or maximum area of the contaminant was defined. Microscopes attached to spectrophotometers working in the infrared region can identify impurities that are in the field of view of the microscope. Scanning of a rocket nozzle with a microscope is probably not practical and a spot of this size would probably not interfere with the formation of an acceptable bond. Two sets of experiments are summarized in this report. For the first experiment described an approximately 1 millimeter circle was observed. For the second set of experiments a circle approximately 1 centimeter was observed.

1. Observations Using a Guided Wave Model 300

The Guided Wave Model 300 predisposes the illuminating beam. The available instrument used a 470 l/mm grating and an extremely sensitive proprietary detector. The scan range was 900 to 1700nm. The illuminating light beam was carried to the sample by a single strand 500 micron optical fiber and was positioned at a 45° to the surface. A small lens on the

end of the fiber collimated the beam to a spot approximately 1 mm in diameter. This spot was observed with a similar lens and fiber and the reactance signal returned to the detector. The macro language developed by Guided Wave, Inc. was used to write a software program to control the spectrophotometer and to drive an X-Y table to examine 100 spots equally spaced on the aluminum block. The spectrophotometer operating at a collection rate of approximately 1200 readings/second recorded the average of 7 spectra at each observation point. The operation was performed in a room with all lights turned off and tape covering the LEDs on the instrument panel. The spectra obtained for 1 pass across the block are shown in Figures 10 and 11. At the scale used in Figure 10 the spectra closely resemble the pattern of random numbers described in the theory discussion. In Figure 11 the readings have been smoothed using a Fourier algorithm that removes frequencies greater than 2 times the observation rate (assumes all bands representing structural features have greater width and that the high frequency information must be random noise) and a Savitsky-Golay 15 point smooth. The spectra in Figure 11 have been offset in both X and Y direction to make it possible to determine the position of a decreased reflection representing an absorbing contaminant. The FACTOR routine in the $SPSS_x$ software package was used to examine the eigenvectors in the 100 point data. A three dimensional plot of the loading factors is shown in Figure 12. As discussed earlier the experimenter must interpret the eigenvectors. The higher points represent the places where the contaminant was placed.

2. Observations using a Guided Wave Model 260

For these experiments a spot on the surface approximately 2 centimeters in diameter was illuminated by focusing the energy from a spot light containing a tungsten halogen bulb. The spot light was at 45° to the surface. A probe placed perpendicular to the surface and containing 6 fibers was use to return the reflected energy to the spectrophotometer where the dispersion occurred and the spectrum determined. A set of data are shown in Figure 13. Since the observed region was larger than the experiments described with the Model 300, Only 6 spectra were recorded. The data in Figure 13 has been smoothed and is shown with offset. The contaminant was a finger print. The spectrum of the finger print can be seen in the tenth scan. The absorption was so intense that the quantity of material was reduced with a solvent. The new spectrum of the finger print is shown as the fourth spectrum. The data shown in Figure 13 is for

the near infrared, NIR. The finger print was also observed in the ultraviolet. Since it is anticipated that the spectroscopic inspection will be synergistic with OSEE spectroscopy, spectra were also recorded using the OSEE lamp. A spectrum is shown as Figure 14.

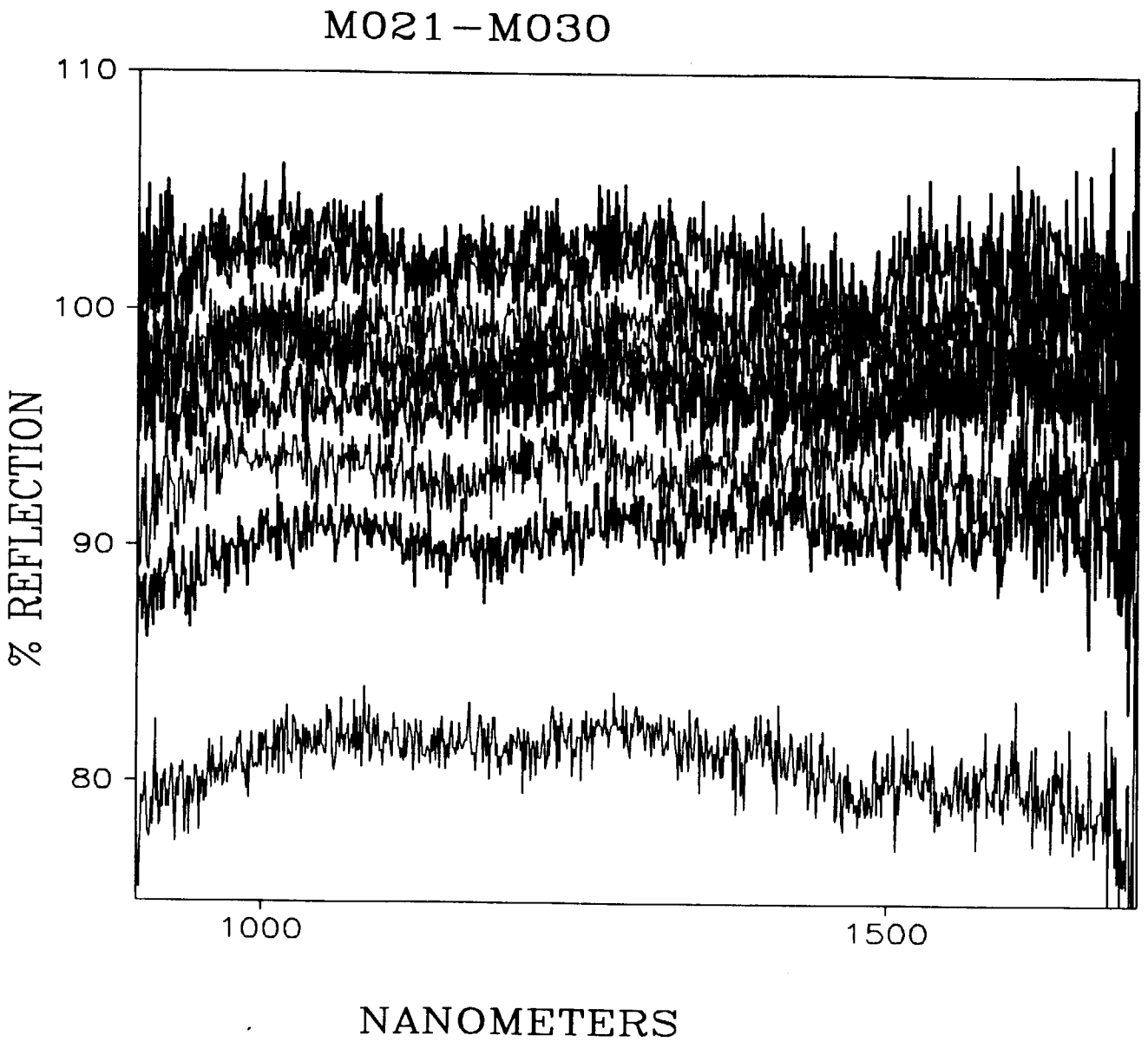

Figure 10. Reflection Spectra 45⁰ - 45⁰

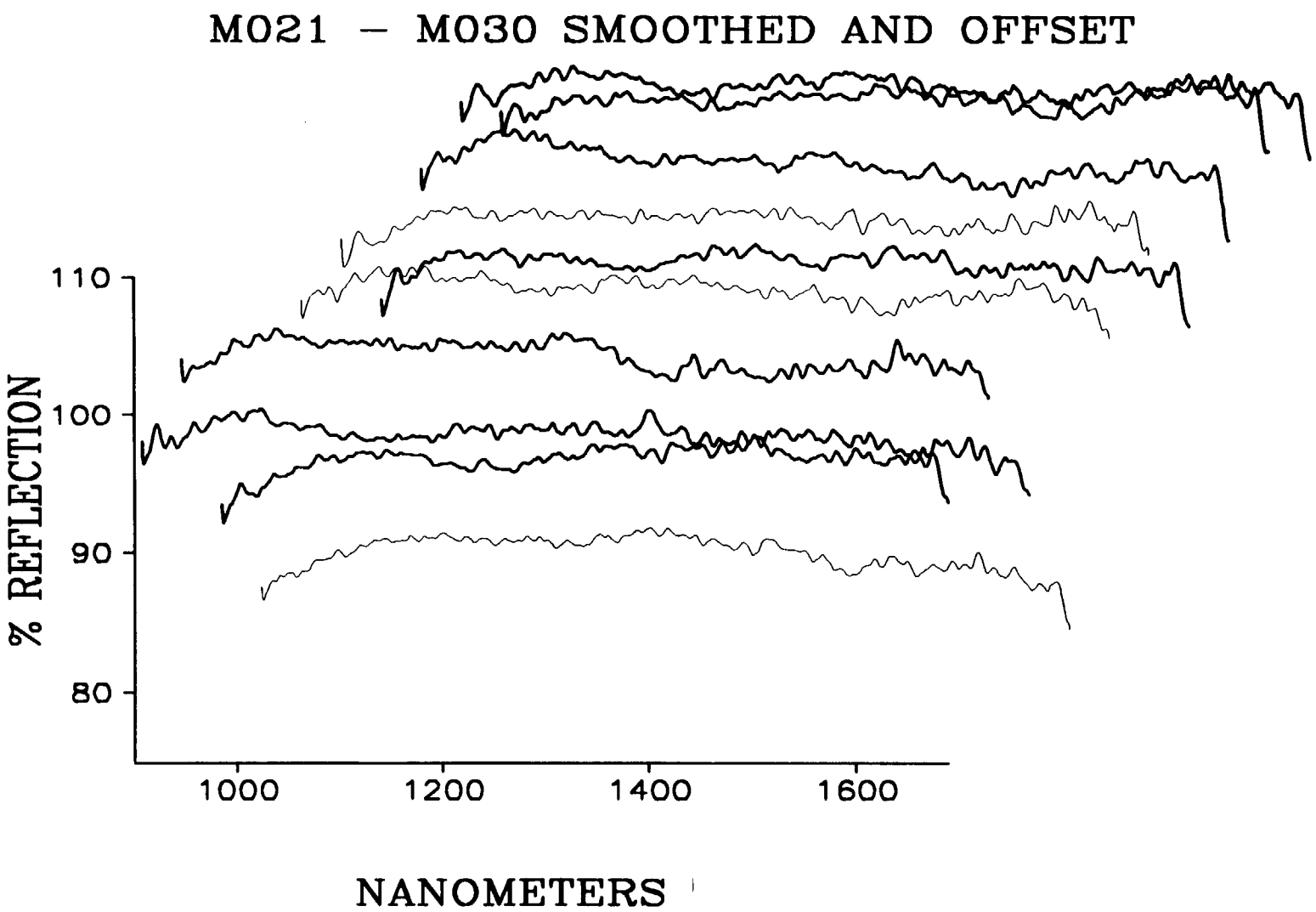

Figure 11. Reflection Spectra After Smoothing

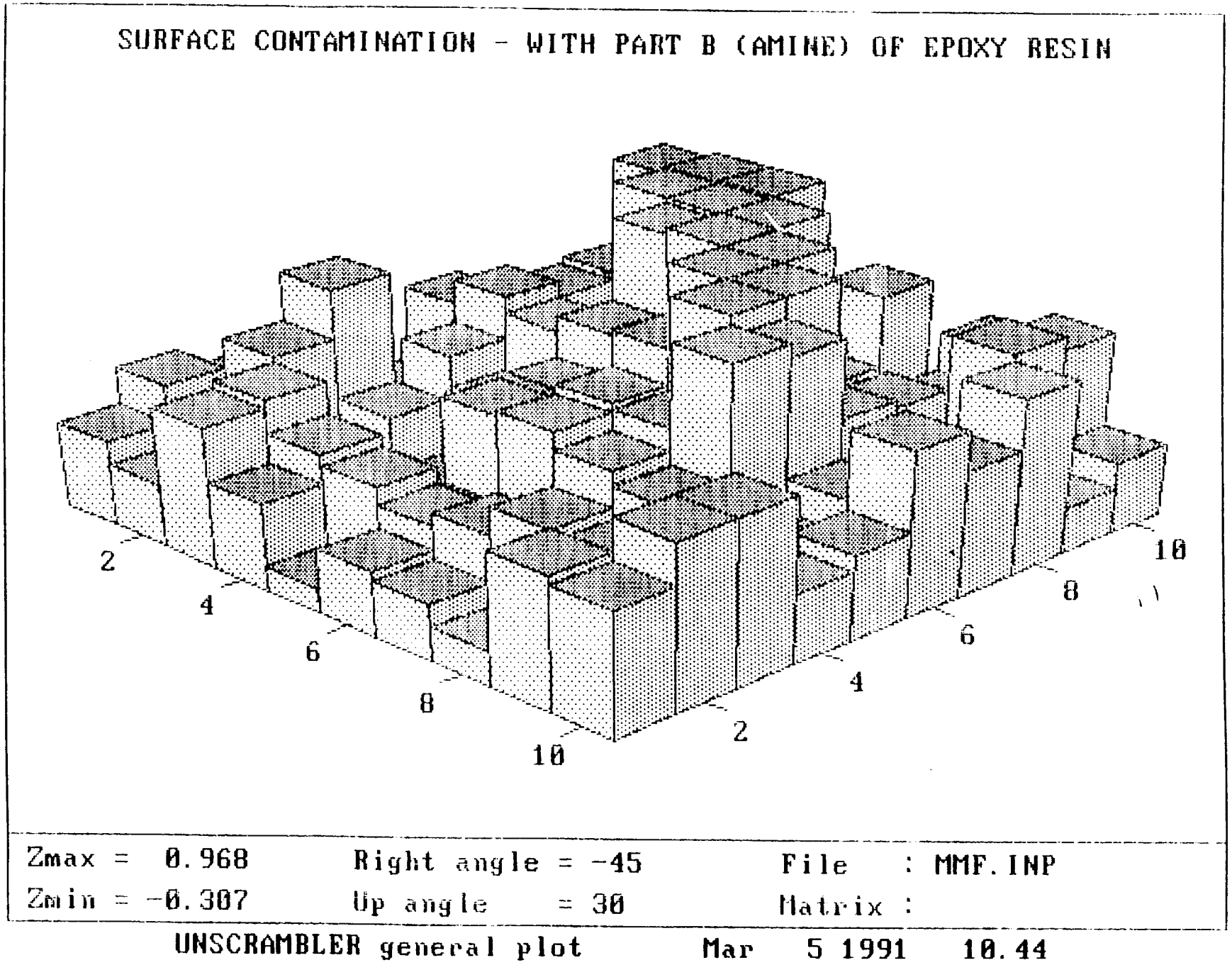

Figure 12. Plot of Amine Factor 1

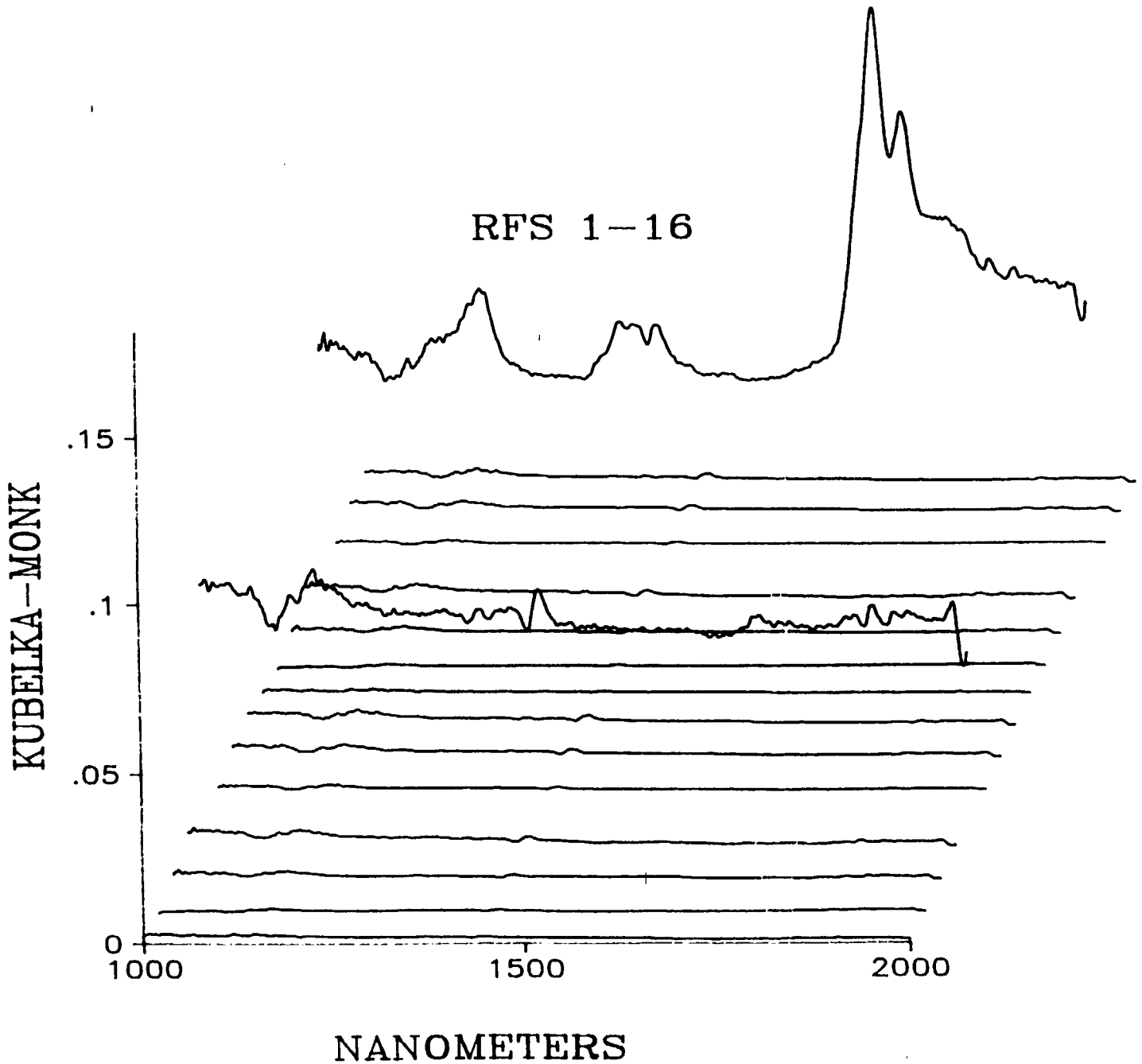

Figure 13. Grease on Aluminum RFS 1-16 Model 260

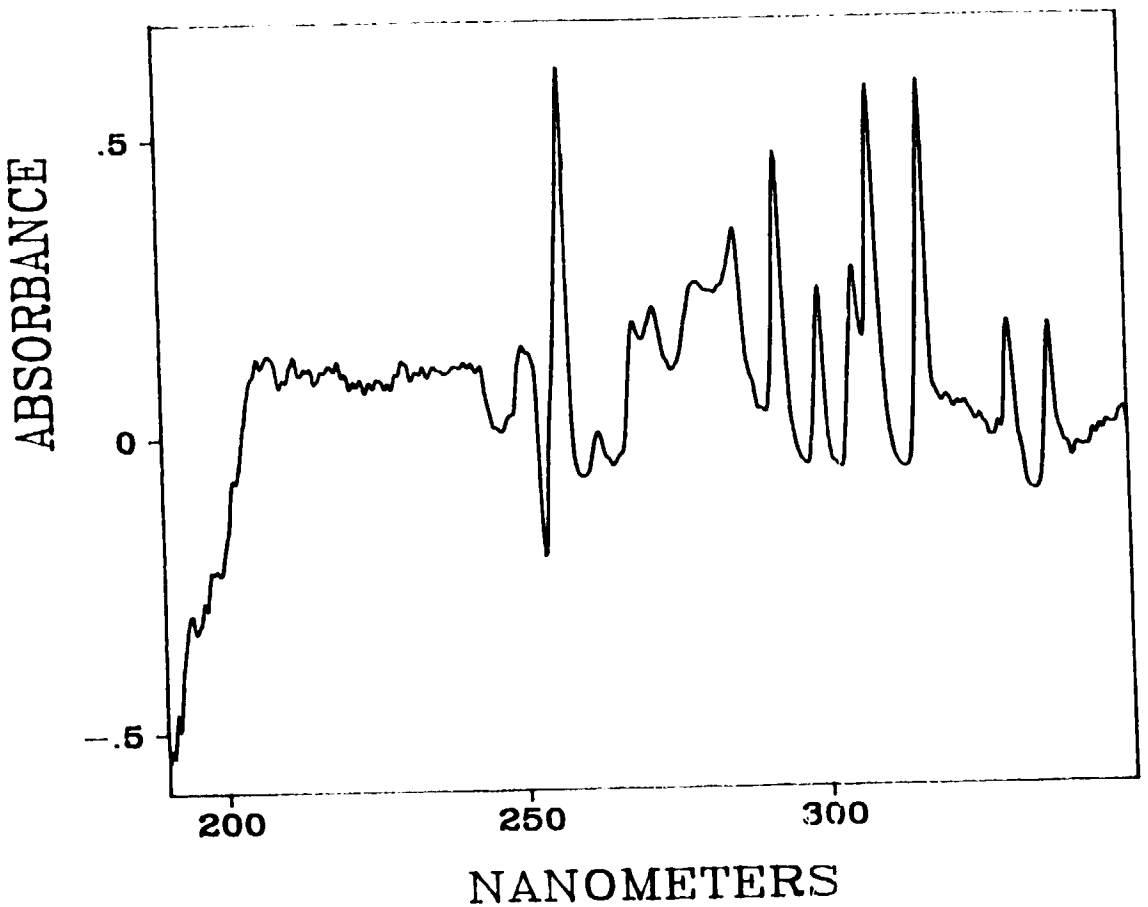

Figure 14. Fingerprint on Aluminum - UV region - Model 260

This experimental setup was also used in an attempt to follow the cure of Hysol EA934NA. Usable spectra were obtained. None of this data is presented because it was obtained early within the program before all of the variables had been investigated. The work reported in the next section indicates that the observed spectrum is very sensitive to the A:B ratio and the temperature. The experimental setup using the high intensity lamp caused the epoxide mixture to turn brown from overheating and the mixtures at this time were being made using a beam balance. It is shown in the section on ATR spectroscopy that an analytical balance, very thorough mixing, and temperature measurement are required in order to obtain reproducible spectra.

3. Conclusions and Recommendations

Two extremes of illumination were investigated. Both gave signatures that could be interpreted. A careful study should be made of the size imperfections that can be tolerated. This will determine the size of the observed spot and the illumination required. The optimum system could be a system that scans quickly with a large spot and then rescans at a smaller spot size to better define the area affected and the composition of the contaminant.

ATTENUATED TOTAL REFLECTION SPECTROSCOPY

A. THEORY

1. Reflection and Refraction of a Beam

When a ray traveling in a low index of refraction medium strikes a non opaque surface of higher index of refraction, some of the light is reflected and some of the light is refracted. This condition is represented in Figure 9.

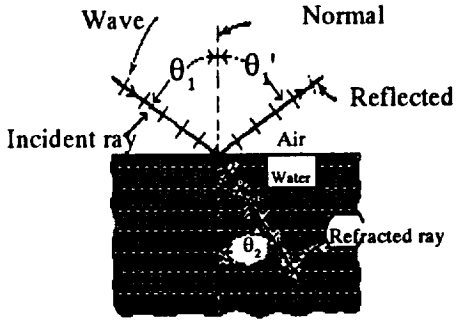

Figure 15. Reflection and Refraction at Air - Water Interface

$$n_{air} < n_{water}$$

θ_1 and θ_1' represent the angle of incidence and the angle of reflection. θ_2 is the angle of refraction. All angles are measured from the normal to the surface. The laws governing reflection and refraction can easily be found from experimentation.

1. The reflected and refracted rays lie in the plane formed by the incident ray and the normal to the surface at the point of incidence.

2. For reflection: $\theta_1' = \theta_1$

3. For refraction, $\sin \theta_1 / \sin \theta_2 = n_{21}$ where n_{21} is a constant called the index of refraction. The index of refraction of one medium with respect to another varies with wavelength. Because of this fact, refraction, unlike reflection, can be used to analyze a beam of light into its component wavelengths. The Laws of Reflection and Refraction can be derived

from Maxwell's equations. These laws should hold for all regions of the electromagnetic spectrum.

The path of a beam traveling in a higher index of refraction medium passing to a medium of lower index of refraction is shown in Figure 16.

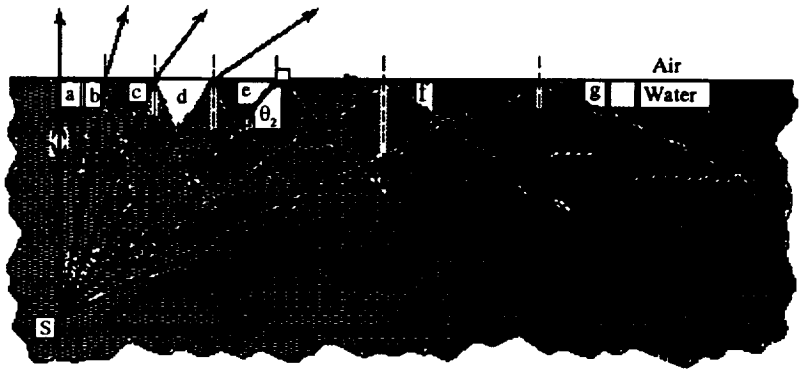

Figure 16. Total Internal Reflection

As the angle of incidence, θ, is increased, a situation is reached (see ray e) at which the refracted ray points along the surface, the angle of refraction being 90°. For angles of incidence larger than this "critical angle", no refracted ray exists, giving rise to a phenomenon called total internal reflection. The critical angle is found by putting $\theta_2 = 90°$ in the law of refraction.

$$n_1 \sin \theta_c = n_2 \sin 90°$$
$$\sin \theta_c = n_2/n_1$$

Total internal reflection does not occur when the ray originates in the medium of lower index of refraction.

2. Multiple Total Internal Reflections

If a ray enters a nonabsorbing rod at an angle greater than the critical angle then the ray can pass through the rod without attenuation. This condition is represented in Figure 17.

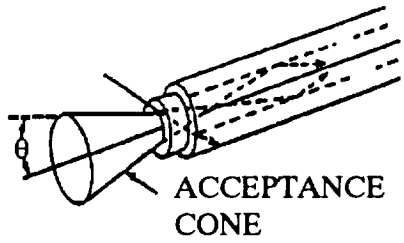

Figure 17. Ray Transmission by Total Internal Reflection

The acceptance angle is defined by the critical angle. The numerical aperture, NA, is calculated by the following formula

$$NA = \sin\theta = \sqrt{n_1^2 - n_2^2}$$
$$n_1 > n_2$$

The cone of light exiting the other end of the rod will be defined by a similar cone. If the entrance cone is smaller than the acceptance cone, the exit cone will usually fill the full cone. If there are bends in the fiber there will be energy losses to the cladding as shown in Figure 18.

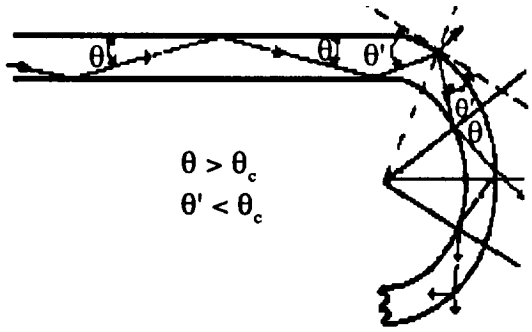

Figure 18. Losses Due to Bend in Fiber

The losses to the cladding represent loss of signal and the cladding modes also perturb the signal. If the cladding modes carry a high percenteage of the energy, the exit cone can appear as a doughnut. Frequently the cladding is removed for a short distance before the detector so that only core radiation reaches the detector.

Probably the single most important parameter related to the performance of optical fibers is the surface between the core and the cladding. If the silica fiber comes in contact with moisture in the air as it leaves the drawing furnace, small cracks form. These cracks reduce tensile strength and decrease signal strength. Fiber is drawn in a moisture free inert atmosphere. The lower index of refraction required for the cladding is often obtained by drawing the fiber into a fluorine atmosphere. This not only removes the OH groups by reaction, but the fluorine diffuses into the quartz providing the desired lower index of refraction coating that serves as the defining cladding. To prevent the penetration of moisture that would cause microcracks which would result in attenuation of signal and low tensile strength in the fiber a buffer is usually added. Polymer coatings, usually proprietary to each manufacturer, are added.

Microbends divert signal energy into cladding modes. Many excellent sensors for measuring microstrain have used this feature. A simple strain sensor is shown in Figure 19.

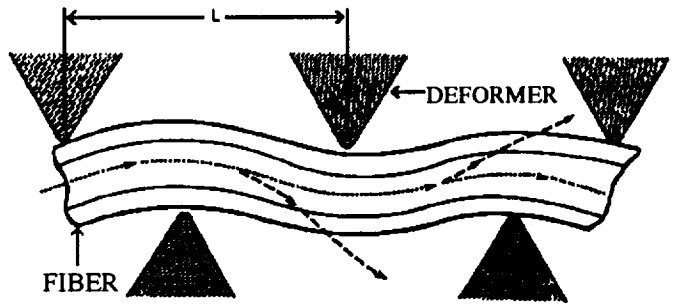

Figure 19. Microstrain Sensor

The attenuation of signal due to microbends represents an almost uncontrollable loss of signal in optical fibers used to connect sensors to the light source and detector. Better precision is obtained when the fiber is supported by cabling. One cable is shown in Figure 20.

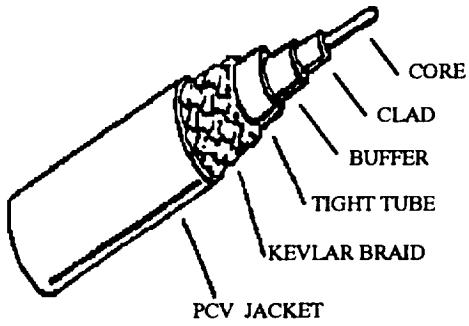

Figure 20. A Complete Cable

The use of uncabled fiber for experiments reported in the literature is believed to be a major factor that prevents reproducibility by other laboratories. When uncabled fiber is used, the fiber should be supported in a fixed position and the sample carried to the fiber. The uncabled fiber should not be moved from sample to sample.

3. Temperature Fluctuations and Microbends

A bend in the fiber causes some of the energy to leave the fiber core and pass into the cladding. As shown in Figure 19 this phenomena can be used to design devices that can measure microstrain. These devices can be used to measure mass when calibrated, can be placed in mechanical models to measure stress distributions, and have been made into instruments to measure acoustics. Errors can be minimized for chemical sensors by use of well-buffered cables that prevent microbends. If possible, we take the sample to the probe so that each measurement is made with the cable in a fixed position. When real-time measurements are being made, a fixed cable arrangement can be used. When movement of the cable cannot be avoided, movement of the cable is included as a variable in the calibration set. Since readings are taken at multiple wavelengths and all wavelengths are not affected proportionally by movement of the cable, the multivariant search methods allot some of the frequencies to the fiber variations while finding other more reliable frequencies to use in quantitating the analytes of interest.

The light beam passes down the fiber core in a number of modes. These modes depend on diameter and length of fiber. As the temperature is raised, a fiber expands in diameter and length causing a change in the magnitude of the signal which is observed. If we are dealing with

low signal to noise ratio, temperature variation can be important. Changes in material properties with temperature are reversible and reproducible. When temperature changes must be included, a temperature measurement is substituted for a wavelength value. A publication described one application where a sensor was excellent for measuring temperature when strain was constant and one wavelength was used. When temperature was held constant, the sensor was excellent for measuring strain using the same wavelength. The solution was simple, use one wavelength to quantitate temperature and a second wavelength to quantitate strain. As we optimize the technique and move toward a minimum number of frequencies we expect to observe the temperature effects.

2. Modification of Cladding

A number of sensors are described in the literature where the sensor consists of a core with a cladding with special properties. In Section A-2 we described the energy rays as passing through the fiber if the light strikes the cladding at an angle greater than the critical angle. It has been shown that although the energy is totally reflected there is an evanescent energy wave that penetrates microinches into the cladding. Reflection is attenuated if the cladding has an absorption band at a wavelength in the illuminating radiation. Many experiments have been devised that demonstrate and use this phenomenon. Most of these designs also use the change in NA associated with the change in the ratio of refractive indices of the core and cladding. Several different arrangements are shown in Figure 21.

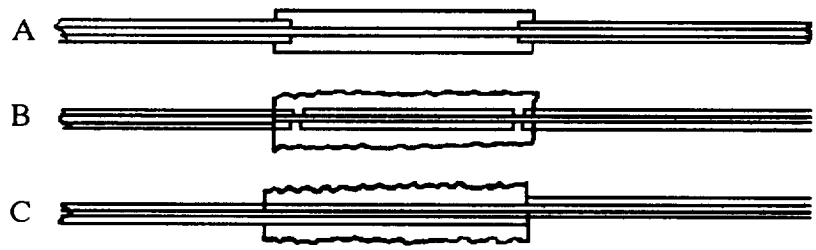

Figure 21. Sensors Designs Using the Evanescent Wave

The sensor shown as A in Figure 21 has the buffer removed and the sample is in contact with the fiber. For this arrangement, the ATR, attenuated total reflection spectra of the sample is recorded. The sensor shown as B has a special cladding placed between the core and sample. If the sample or a component of the sample is absorbed by the cladding, the ATR spectrum is obtained as this analyte reaches the core. If the sample is soluble in the cladding the cladding will swell. If the sample has a higher index of refraction than the cladding material, then n_2 may become greater than n_1 and all energy may be absorbed. The sensor shown as C has the core of one fiber terminated within the sample. A second core is placed next to the fiber bringing the light into the sample region. This second fiber picks up portions of the energy. This twin core type of sensor can be used for special types of analytes. ATR has been used frequently in the infrared region from 3 to 25 microns. Most manufactures of FTIR and dispersion spectrophotometers and several third party dealers sell accessories for ATR. Since waveguides for this region of the electromagnetic spectrum depends on mirrors to define the light path, the active element similar to the one shown in Figure 22 is used.

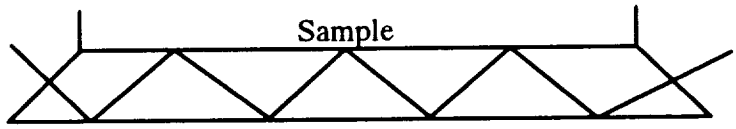

Figure 22. ATR Plate

If a sample is spread across the top of the plate, the evanescent wave would interact with the sample 3 times. Each manufacturer has his specific design. Since the depth of the penetration is related to the ratio of the index of refraction of the crystal and the sample, many speciality designs are available.

For D.O. 107 a probe, Guided Wave Part No. 1AT4 50-6B has been used. This probe is approximately 6 inches in length. Two optical fibers pass down the stainless steel probe. One fiber is used to pass light in and the second returns the reflected signal. Mounted at the end of

the probe is a sapphire crystal. The light beams undergoes 3 reflections before reaching the fiber that return the light to the spectrophotometer.

B. EXPERIMENTAL RESULTS

1. Approach

The work statement for D. O. 107 required that many possible combination should be considered. The end objective is to correlate spectral signatures obtained during the manufacturing process with physical properties of the final bond. A proper bond requires a properly prepared surface. For the examination of surfaces, the use of reflection spectroscopy was investigated. As indicated in the previous section near Lambertian reflection patterns were observed for the aluminum test pieces that were provided. The intensity of the light coming from the surface in a given direction is a small part of the total reflected radiation. Although the signal is small it can be used to the observers advantage. As explained earlier the reflection often has a peak in the direction of the specular reflection. If the objective is to measure the characteristics chemical signature of the very thin layer of material on a surface, the path length as the light passes through the contaminating, layer is reflected at the surface, and then passes a second time through the absorbing material is short. The absorbance, the logarithm of the ratio of the magnitude of the absorbed energy to the magnitude of the illuminating energy provides an advantage but with the associated disadvantage of low signal/noise ratio. If the observation probe is placed at the position of the specular radiation, large variations are observed if the contaminate fills in the rough spots making the surface appear as a mirror. The best results during this investigation were obtained with the illumination at 45^0 and the signal probe normal to the probe.

When the mixture of parts A and B of the Hysol 934NA were examined, two additional variants were observed. If illumination was at 45^0 and the signal was measured 90^0 away at the reflection angle very critical adjustment of the probe's distance from the sample was required. This was very critical when using the previously described 1 mm collimated beams. Although

excellent spectra were obtained, it is doubtful that this arrangement could be developed into a practical method for inspecting large and curved surfaces. The experimental arrangement where the resin mixture was illuminated using a large lamp focused on a spot approximately 2 cm in diameter and a collimated beam 1 cm in diameter at 45^0 to the normal normal to surface was used. Again usable spectra were obtained. However, the surface was observed to become increasingly resin rich with time. The optical components that were used caused the resin to turn brown from overheating.

Throughout the investigation both reflection spectroscopy and attenuated reflection spectroscopy were alternately being investigated. The signal/noise ratio for ATR spectrum is similar to reflection spectrum. When the ATR probe is placed in the mixture the sapphire crystal becomes wetted by the resin mixture that migrates through the filler to the crystal surface. Therefore, the ATR spectrum is sensitive to the viscosity of the mixture at the time the probe is placed in the sample. When the probe was placed in the sample and a series of measurement made without moving the probe, consistent spectrum could be obtained. Time was not available to make another circle through the various experimental parameters. Therefore for the remainder of this report we concentrate on those attributes about which we obtained what we beleive is the most useful information.

2. Results From a Study Using the ATR Probe

Temperature effects viscosity, a variable that has an effect on measured spectra. Also temperature affects the rate of chemical reaction. Temperature is an effect that is readily measured and controlled. Even in an air conditioned laboratory the ambient temperature varies several degrees from day to day. The temperature of the adhesive components at the time of mixing was varying depending on the elapsed time from removal from the refrigerator and the initiation of experiments.

A quality multichannel thermistor thermometer with two fast response probes was used. One probe was used to measure ambient temperature and the other probe was used to measure

the temperature of the mix. The relative humidity of the room was recorded for each experiment. This data has not been used as a variable, however, due to the dubious accuracy and the fact that it never varied more than a few percent day-to-day in the air conditioned laboratory environment.

Multivariate analyses using SpectraCalc PLSPLUS PCR routines were performed using temperature as an added component. The predictive results were less than anticipated. Calibrations looked adequate with reasonably good actual vs. predicted times of cure but the calibration matrix had little predictive value for subsequent tests. Interestingly the temperature values for the calibration, actual vs predicted, were substantially poorer than the time predictions in the calibration set. This may be in part due to the non-linear behavior of temperature during cure. Freshly mixed adhesive is at a temperature maximum due to the heat generated during mixing. The temperature in the small laboratory samples drops rapidly as the heat is lost to the environment. After 35 to 50 minutes the temperature almost always rises slightly, or at least a plateau is reached as some secondary thermal process becomes dominant until the temperature begins dropping toward ambient once again. Data for several mixtures is shown in Figure 22. This behavior was especially pronounced during a low temperature curing experiment where the container containing the mixture was placed in a cooling bath during the period of observation. The data is shown in Figure 23.

From the temperature dependent data analysis it became apparent that there were significant spectral variations run to run even when temperature and time variables were closely monitored and procedural techniques were as refined as seemed practical at the time. Individual scans of the mixtures of part A and B of the adhesive at different ratio had been taken throughout the investigation to try to understand spectral features in terms of chemical functional groups. Review of these spectra hinted that small variations in mixing ratio might account for the significant but unexplainable spectral differences that where being observed in the multivariate analysis.

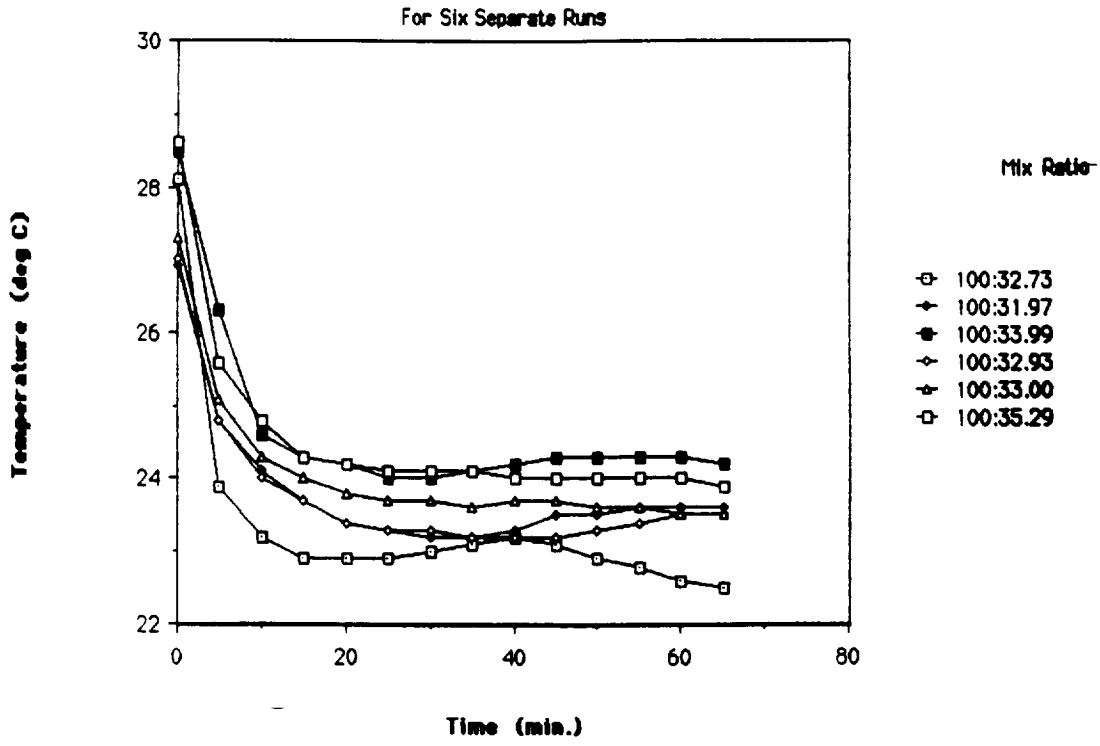

Figure 22. Temperature vs. Time

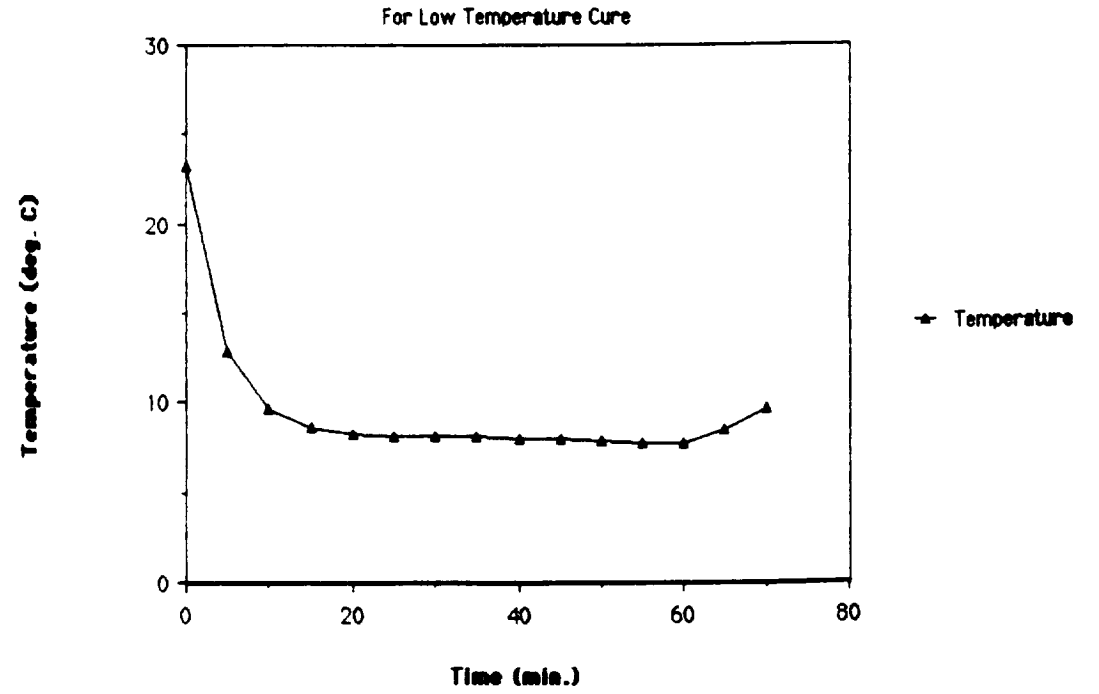

Figure 23. Temperature vs. Time

3. Laboratory Demonstration of ATR Procedure

An analytical balance was procured and used to determine the mix ratio of parts A to B to a high degree of accuracy. (Previously a beam balanced had been used.) An even more exacting, controlled methodology was adopted to control unknown variables as much as possible. The Hysol 934NA epoxide resin and catalyst were allowed to come to room temperature overnight, and the spectrometer source lamp was allowed to stabilize at least 4 hours. Ambient temperature and humidity were recorded prior to each experiment. The tare weight of the small polycarbonate mixing dish was recorded. The same vessel was used for weighing, mixing, and observing cure so no transfer losses or errors were possible. Approximately 10 grams of resin (part A) was weighed to the nearest milligram. A quick ratio calculation determined the "target" amount of amine (part B) to be added to produce the desired mix ratio. Then the amine was added to the weighing dish. The actual ratio is later calculated to 6 significant figures (100:33.0039). Immediately after the amine was added and the total weight was recorded. The two parts were mixed with a stainless steel spatula very thoroughly and completely for exactly 5 minutes (using a timer) so that a homogeneous mixture is practically assured. This sample was immediately transferred to the optics stage, the ATR probe and thermistor were inserted and data acquisition started. One scan was taken immediately and automatically every 5 minutes thereafter. Pot temperatures were recorded manually at the start of each scan.

The data from this study indicate that mix ratio had not been sufficiently controlled weighing 10.0 grams of A and 3.3 grams of B on a beam balance. Small variations in mix ratio (1 or 2 parts in 133 parts total) has a pronounced effect on spectral features.

A fifty sample training set was constructed using PCR in the Spectra Calc PLSPLUS software. Three objects were used. Object 1 is pot life or time in minutes after mixing. Object 2 is the pot temperature at the beginning of each scan. Object 3 is the amine (part B) portion of the mix ratio, normalized so that the resin (part A) always equally 100. parts. The training set was constructed using roughly every other scan from six runs with 14 scans each. First, third,

fifth, etc. from the first run were combined with second, fourth, sixth, etc. scans from the next set, and so on, along with a few consecutive scans at random to reach 50 total scans.

The time equals zero scans taken immediately after mixing are quite different in appearance from subsequent scans, probably due to time delay in wetting the surface of the probe (possibly caused by differences in viscosity of the high viscosity mixtures). These scans were removed from the training set.

With this large training set, entire spectra could not be used without over running memory in the Compaq being used (2 MB). Baseline least squares fit normalization was performed on the 1.64 to 2.33 micron region which appeared visibly to have the greatest variance. The calibration diagnostics produced by this training set are very encouraging. RMS prediction error for pot time is 3.3 minutes with a R^2 of 0.96863 (1.0 is a prefect fit). The mix ratio predictions gave a RMS prediction error of only 0.22 parts in approximately 133 parts and a R^2 of 0.952465. The model had trouble with pot temperature predictions, but strangely, eliminating these data as objects slightly deteriorated the model's predictive ability for mix ratio.

4 Demonstration of ATR Procedure in NASA Laboratories

On October 16. 1991 the Guided Wave Model 260 spectrophotometer and the computer were taken to an ED34 Polymer Laboratory in Building 4612. The equipment was set up and calibrated. A test plan was prepared to validate the ability to predict the mix ratio and the tensile strength of cured test specimens. The test were delayed until October 10, 1991 because there were an insufficient number of test pieces to do the experiment as planned. The tests were performed October 22, 1991. Seven mixes were prepared for the calibration set. The mix ratios included the range of 100:25 to 100:43 with duplicate mixes made at the recommended 100:33 ratio. Two additional mixes were prepared as unknowns to the UAH investigator. The adhesive mixtures using 50 g of Part A were weighed into and mixed in a 500 ml disposable beaker (Nalgene). The samples were mixed for 5 minutes (timed). A 20g sample was placed in a small aluminum "hardness test cup" and 5 NIR spectra were taken at 5 minute intervals using the ATR immersion probe. Three specimens were prepared from each batch for tensile testing. The

tensile specimens were cured for 1 week at ambient. SFC personnel were responsible for all operations with the exception of the NIR spectra.

HYSOL 934 NA Lot# 1156-1 was used for the test. This lot was received at SFC on July 10, 1991. Two adhesive kits had been removed from the refrigerator on 8/21/91. Vacuum mixing was attempted for the first sample using lot 1156-1 removed from the refrigerator. 8/21/91. The sample cured so fast that no further test were made on this sample. Subsequent samples using a kit removed from storage 10/22/91 were prepared by hand mixing without vacuum. Sample temperatures were approximately 25° C and only small changes in temperature were recorded during the 25 minutes that the spectra were taken.

Spectra Calc PLS Plus PCR was used to process the Spectra data. A report for the training set is reproduced as APPENDIX 1. The regression curves for tensile strength and mix ratios plotted predicted vs actual using the calibration set data are shown as Figures 24 and 25. The actual vs predicted values for tensile strength and mix ratio for the 2 unknowns are shown in Table 1.

These results indicate that an ATR immersion probe is significantly more sensitive than the current test. The probe can be used to study process variable with greater precision than has been previously possible. The spectrophometric technique can be developed into very sensitive materials acceptance tests and can be used for real time analyses related to process variables.

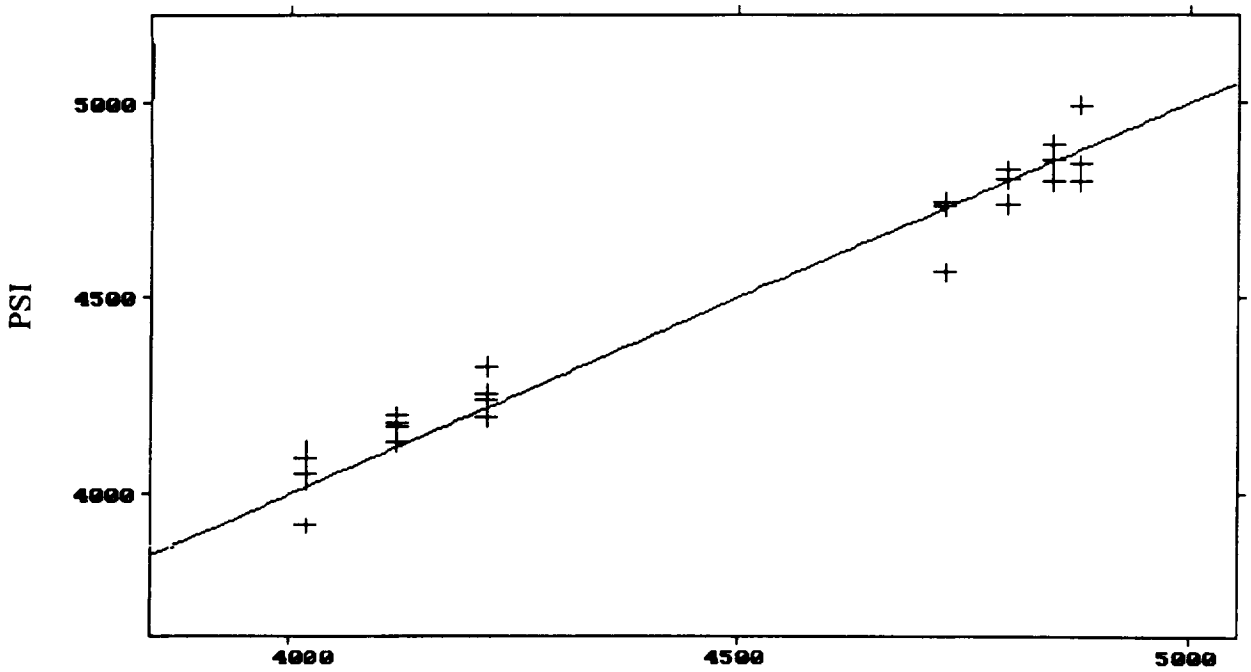

Figure 24. Predicted Tensile Strength vs Measured

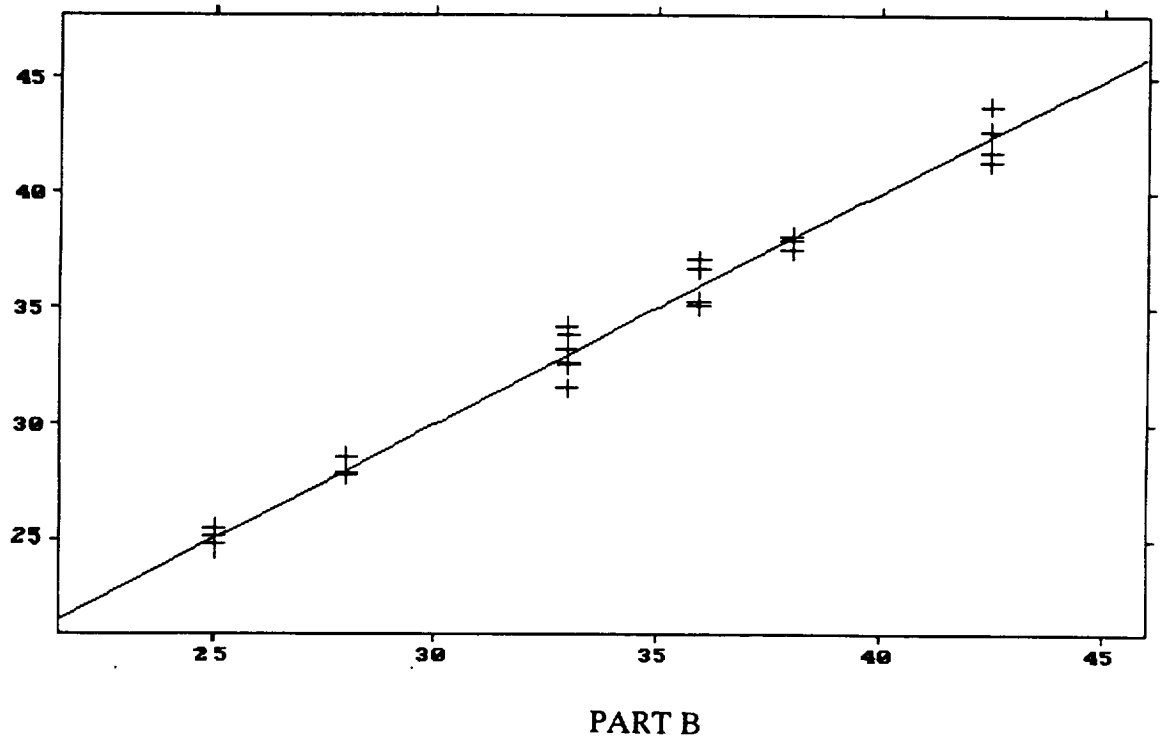

Figure 25. Predicted Mix Ratio 100 A:B vs Actual

Table 1

RESULTS FROM UNKNOWN MIXES

Date 11/12/1991 Quant. Method: PCR

	TEST VALUES	PREDICTED VALUES			
		nasa_72	nasa_73	nasa_74	nasa-75
Modulus	4900 ± 560	4773.57	4773.85	4765.14	4714.55
Mix Ratio	34.1	32.6366	32.6581	32.5197	32.9822

Predicted Modulus 4757± 28.5
Predicted Mix Ratio 32.7 ± 0.2

	TEST VALUES	PREDICTED VALUES			
		nasa_82	nasa_83	nasa_84	nasa_85
Modulus	4470 ± 510	4010.73	4082.47	4105.51	4113.83
Mix Ratio	39.9	40.291	39.4419	39.3276	38.6252

Predicted Modulus 4078 ± 40.6
Predicted Mix Ratio 39.42 ± 0.6

SUMMARY AND RECOMMENDATIONS

Remote spectrophotometry where fiber optics are used to connect a light source to a transducer placed in or on a sample, or to illuminate the sample, and the same or a second fiber optic is used to return a light signal to a spectrophotometer is a rapidly advancing technology in the industrial community. D.O. 107 under contract NAS8-36955 from Marshall Space Flight Center provided that the UAH Laboratory For Inline Process Analyses would investigate the applicability of these techniques as related to bond-line quality where the adhesive is Hysol 934 NA. Permutations of transducers, fiber type, spectral regions, and spectrophotometric techniques were to be investigated. Multivariate analysis techniques would be investigated as methods for correlating measurable properties with measurements using non-destructive tests where the destructive test could not be used on the final product. Recommendations for specific combinations to be tested at Marshall would be provided.

Personnel at UAH began with very little experience with Hysol 934 NA. Hysol 934 NA is a room temperature curing epoxide resin using an amine hardener. Shelf life is limited to one year at 40° F and pot life is limited to 40 minutes after mixing. The short shelf life and pot life were found to have advantages and disadvantages for this study. The short pot life allows several experiments to be performed each day when studying some parameters for example the effect of mix ratio on reaction rate. However, the short shelf life leads to serious questions related to equivalency of raw material samples. Initially UAH was furnished three samples.

Lot No.	Date of Manufacture
8118	4/22/88
9068	3/9/89
0078-1	3/19/90

All of the samples had been stored in the refrigerator at NASA since receipt. Lot 0078-1 was within shelf life limits. The quart containers had not been opened at NASA. Chemistry of epoxide polymers indicate that the epoxide resin can react with itself and with water. The reaction of the epoxide with an amine is much faster.

Initial examination of the samples indicated part A, the epoxide portion, of the sample from Lot 8118 was very hard and therefore only limited tests could be performed. This is strong evidence that reactions are taking place during storage. Part A of sample 9068 was considerably more viscous than part A of sample 0078-1. The wetting properties of the material decreases with increasing viscosity. Part A contains a high percentage of solids. The material is sufficiently viscous that settling of solids has been minimized. Part B, the amine, is very fluid and has little or no suspended matter. When part A is mixed with part B the resulting mixture made from material within shelf life can be readily spread on a surface. There is evidence that the surface becomes resin rich very quickly. Early experiments did not provide the precision or the evidence of reactions that had been anticipated. The materials we were using were probably not typical of materials as used during the actual manufacturing process. A sample from Lot 0269-1 manufactured 9/26/90, received at Marshall on 11/5/90 was delivered to UAH on 4/11/91 was provided. This lot was being used successfully in Marshall test. When experiments were repeated using this sample, data began to follow expected patterns. For the period 4/11/91 to 9/30/91 when the sample was used up the can had been opened many times exposing the resin to laboratory humidity. When the sample was removed from the refrigerator and sampled immediately, small amounts of water may have condensed in the can. It can not be denied that the reactions responsible for shelf aging may have been accelerated. The least reliable of the predictions that we were able to make during this D.O. using the multivariate analyses procedures are related to shelf life. Our data also suggest that as the material ages and becomes more viscous that some of the variance in observations is due to incomplete mixing of part A and B.

The Laboratory For Inline Process Analyses has examined surfaces for contaminants, shelf life, mixing procedure, and mix ratio. Data has been obtained using reflection spectrophotometry and attenuated total reflection, ATR, spectrophotometry. The demonstration performed by MSFC and UAH personnel indicates that an extremely sensitive tool for studying specification and process variables has passed the demonstration phase.

The goal is to obtain **Y** values (predicted values) as a function of **X** (measured values). We envision a probe being used to obtain spectral signatures for the raw materials. The same or a related probe may be used to measure the properties of the mixed material. Reflection spectrophotometry may be used to examine the quality of the prepared surface and the surface after the mixture is in place but preceding placement of the plastic insert into the nozzle. Measurements can be used in the **X** matrix at one stage to predict a value of **Y** for the following stage in the process. If that **Y** parameter can be measured in the following stage then it becomes part of the **X** data vector for predicting **Y** for the next stage. It is likely that parameters will be discovered that can never be dropped from the prediction equation (X matrix). For an example, the spectrum of the part A as received will probably be required at any stage to have a complete predictor matrix for of the mechanical properties of the final bond.

The approach to quality management using pattern recognition algorithms is to gather objects available at each step in the process; make a wide variety of measurements on these objects; find which measurements are useful; and then to develop prediction/classification models that permit the operator to infer values for the properties of the next step in the process and ultimately of the final product where the properties of the deliverable cannot be measured.

Personnel at The UAH Laboratory For Inline Process Analyses have obtained sufficient experience with the chemical properties of Hysol 934NA that they recommend that the acquisition of additional data for an intelligent database should proceed.

As an initial suggestion to be considered by MSFC it is suggested that at least 4 quart samples for each of 4 lots of Hysol 934NA be obtained. One can from each lot will be opened and divided into six parts. Test will be made once a month using the six samples. A detailed log will be kept of temperature, dates when a can is opened, and laboratory humidity and temperature. A second, third and fourth series would be started one month apart.

Mixing conditions must be carefully controlled. It is extremely important that the data set contain some reject material (poor bonds) and non acceptable but previously observed variations in operating practice that produced unacceptable bonds. The final **Y** matrix will include quantities that can not be measured on the final product but have been measured using destructive test procedures on test pieces. The study should also include some specimens that can be used to define minimum unbonded area that results in rejected parts. Tests should be carried out to obtain data for a minimum period of 6 months and preferably to the limit of shelf life for the selected lots.

APPENDIX 1

Experiment Summary Taken from nasa.RPT

Type:	PCR	#Spectra:	25	#Components:	4
#Regions:	1	Sampling:	Skip	#Points:	290
Variance Scaling:	NO	Mean Center:	NO	MSC:	NO
Pathlength Corrc:	NO	Baseline:	YES	Custom:	NO

Number of factors for PRESS: 13 Number of samples for rotation: 1
Name of Method file: nasa.mth Name of Calibration file: nasa2.CFL

Number of factors for Calibration: 6

Region #	Left edge	Right edge	Pt spacing	# points
1	1650	2230	2	581

Components	RMS Pred. Error	R squared
Compnt4	69.8309	.961388
Compnt1	7.52746	0
Compnt2	.486881	.682975
Compnt3	.634486	.987449

PRESS values (PCR).

Factor#	PRESS	F calc	Prob {F<=Fc}
0	3158876	28.8783	1
1	3329617	30.4392	1
2	732813	6.69935	.999958
3	792083	7.2412	.999972
4	657594	6.0117	.999925
5	752095	6.87563	.999964
6	123341	1.12758	.614634
7	112333	1.02694	.525517
8	109385	1	.5
9	115376	0	0
10	114289	0	0
11	109585	0	0
12	111156	0	0
13	146712	0	0

Concentration prediction for component Compnt 4 using 6 Factors (PCR).

Sample#	Name	Actual	Predicted	Differ	Error(%)	SpecResid(%)
1	nasa_12	4850	4850.2	-.2666	-.0054969	3.0741
2	nasa_13	4850	4893.8	-43.857	-.90428	2.8691
3	nasa_14	4850	4853.1	-3.1875	-.065721	3.009
4	nasa_15	4850	4798	51.924	1.0706	3.8419
5	nasa_22	4020	3866.9	153.04	3.807	5.4481
6	nasa_23	4020	3925.5	94.433	2.3491	6.6656
7	nasa_24	4020	4053.4	-33.446	-.83199	4.702
8	nasa_25	4020	4089.2	-69.226	-1.722	5.3525
9	nasa_33	4730	4744.8	-14.875	-.3145	5.566
10	nasa_34	4730	4732.7	-2.7583	-.058315	7.3273
11	nasa_35	4730	4563.5	166.47	3.5195	5.6138
12	nasa_43	4800	4737.1	62.844	1.3092	3.8626
13	nasa_44	4800	4825.2	-25.259	-.52623	3.6425
14	nasa_45	4800	4801.3	-1.3129	-.027353	3.3815
15	nasa_52	4120	4131.6	-11.624	-.28214	4.9756
16	nasa_53	4120	4169.3	-49.303	-1.1966	3.7006
17	nasa_54	4120	4182.7	-62.723	-1.5224	4.5174
18	nasa_55	4120	4198	-78.036	-1.894	6.0217
19	nasa_62	4880	4797.5	82.458	1.6897	4.4077
20	nasa_63	4880	4840.1	39.865	.81692	4.8189
21	nasa_65	4880	4992.5	-112.52	-2.3058	4.5141
22	nasa_92	4220	4193.9	26.063	.61761	3.6165
23	nasa_93	4220	4238.7	-18.767	-.44471	3.3591
24	nasa_94	4220	4254.4	-34.407	-.81534	3.052
25	nasa_95	4220	4323.1	-103.14	-2.4442	2.8434

Concentration prediction for component Compnt1 using 6 Factors (PCR).

Sample#	Name	Actual	Predicted	Differ	Error(%)	SpecResid(%)
1	nasa_12	5	16.542	-11.542	-230.85	3.074
2	nasa_13	10	14.602	-4.6023	-46.023	2.8691
3	nasa_14	15	12.233	2.7666	18.444	3.009
4	nasa_15	20	9.0516	10.948	54.741	3.8419
5	nasa_22	5	13.914	-8.9143	-178.28	5.4481
6	nasa_23	10	12.67	-2.67	-26.7	6.6656
7	nasa_24	15	12.773	2.2263	14.842	4.702
8	nasa_25	20	10.83	9.1698	45.849	5.3525
9	nasa_33	10	25.171	-15.171	-151.71	5.566
10	nasa_34	15	13.433	1.5666	10.444	7.3273
11	nasa_35	20	13.529	6.4701	32.35	5.6138
12	nasa_43	10	17.642	-7.642	-76.42	3.8626
13	nasa_44	15	14.739	.26048	1.7365	3.6425
14	nasa_45	20	12.884	7.1157	35.578	3.3815
15	nasa_52	5	12.973	-7.9737	-159.47	4.9756
16	nasa_53	10	10.922	-.92218	-9.2218	3.7006
17	nasa_54	15	10.565	4.4346	29.564	4.5174
18	nasa_55	20	8.8289	11.171	55.855	6.0217
19	nasa_62	5	15.018	-10.018	-200.37	4.4077
20	nasa_63	10	12.658	-2.6581	-26.581	4.8189

21	nasa_65	20	11.916	8.0834	40.417	4.5141
22	nasa_92	5	15.454	-10.454	-209.08	3.6165
23	nasa_93	10	14.474	-4.4747	-44.747	3.3591
24	nasa_94	15	13.253	1.7468	11.645	3.0522
25	nasa_95	20	12.167	7.8325	39.162	2.8434

Concentration prediction for component Compnt2 using 6 Factors (PCR).

Sample#	Name	Actual	Predicted	Differ	Error(%)	SpecResid(%)
1	nasa_12	22.1	21.599	.50065	2.2654	3.0741
2	nasa_13	21.8	21.721	.078636	.36071	2.8691
3	nasa_14	21.7	21.697	.0023555	.010855	3.009
4	nasa_15	21.5	21.94	-.4409	-2.0507	3.8419
5	nasa_22	23.4	22.602	.79783	3.4095	5.4481
6	nasa_23	22.6	22.834	-.23402	-1.0355	6.6656
7	nasa_24	22.2	22.549	-.34902	-1.5721	4.702
8	nasa_25	21.9	22.307	-.40735	-1.86	5.3525
9	nasa_33	22.5	21.629	.8707	3.8698	5.566
10	nasa_34	22.1	22.114	-.014894	-.067395	7.3273
11	nasa_35	22.1	22.4	-.30007	-1.3577	5.6138
12	nasa_43	23.6	23.115	.48437	2.0524	3.8626
13	nasa_44	23.1	23.158	-.058752	-.25433	3.6425
14	nasa_45	22.8	23.088	-.28856	-1.2656	3.3815
15	nasa_52	24.7	23.786	.91307	3.6966	4.9756
16	nasa_53	23.9	23.731	.16818	.7037	3.7006
17	nasa_54	23.4	23.544	-.14458	-.61788	4.5174
18	nasa_55	23.1	23.977	-.87734	-3.798	6.0217
19	nasa_62	21.9	21.679	.22005	1.0048	4.4077
20	nasa_63	21.5	21.702	-.20219	-.94043	4.8189
21	nasa_65	20.9	21.314	-.41485	-1.9849	4.5141
22	nasa_92	23.4	22.428	.97174	4.1527	3.6165
23	nasa_93	22.6	22.404	.19598	.86718	3.3591
24	nasa_94	22.2	22.569	-.36929	-1.6634	3.0522
25	nasa_95	21.9	22.441	-.54143	-2.4723	2.8434

Concentration prediction for component Compnt3 using 6 Factors (PCR).

Sample#	Name	Actual	Predicted	Differ	Error(%)	SpecResid(%)
1	nasa_12	25.05	25.264	-.21462	-.8568	3.0741
2	nasa_13	25.05	24.834	.2151	.85868	2.8691
3	nasa_14	25.05	25.11	-.060718	-.24238	3.009
4	nasa_15	25.05	25.382	-.3323	-1.3265	3.8419
5	nasa_22	42.47	43.622	-1.1526	-2.714	5.4481
6	nasa_23	42.47	42.592	-.12252	-.28848	6.6656
7	nasa_24	42.47	41.774	.69574	1.6382	4.702
8	nasa_25	42.47	41.265	1.2048	2.8368	5.3525
9	nasa_33	32.99	33.517	-.52744	-1.5987	5.566
10	nasa_34	32.99	31.96	1.0292	3.1198	7.3273
11	nasa_35	32.99	33.902	-.91221	-2.7651	5.6138
12	nasa_43	28	28.53	-.53085	-1.8959	3.8626
13	nasa_44	28	27.805	.19407	.69313	3.6425
14	nasa_45	28	27.82	.17974	.64193	3.3815

15	nasa_52	38.04	38.17	-.13071	-.34363	4.9756
16	nasa_53	38.04	38.102	-.062896	-.16534	3.7006
17	nasa_54	38.04	37.446	.59397	1.5614	4.5174
18	nasa_55	38.04	38.029	.010982	.02887	6.0217
19	nasa_62	33.01	33.85	-.84079	-2.547	4.4077
20	nasa_63	33.01	32.736	.27328	.82789	4.8189
21	nasa_65	33.01	32.823	.18668	.56553	4.5141
22	nasa_92	35.96	37.08	-1.1202	-3.1151	3.6165
23	nasa_93	35.96	36.66	-.70092	-1.9491	3.3591
24	nasa_94	35.96	35.322	.63761	1.7731	3.0522
25	nasa_95	35.96	35.115	.84499	2.3498	2.8434

REFERENCES

1. See D. L. Massart, A. Dijkstra, and L. Kaufman, *Evaluation and Optimization of Analytical Procedures*, Elsevier, Amsterdam, 1978; Edmund R. Malinowski and Darryl G. Howery, *Factor Analysis in Chemistry*, John Wiley and Sons, New York, 1980; D. Luc Massart and Leonard Kaufman, *The Interpretation of Analytical Chemical Data by the use of Cluster Analysis*, John Wiley and Sons, New York, 1983; Muhammad A. Sharo, Deborah L. Illman, and Bruce P. Kowalski, *Chemometrics*, John Wiley and Sons, New York, 1986; D. L. Massart, B. B. M Vande-

2. E. R. Malinowski, D. G. Howery, P. H. Weiner, P. T. Soroka, p. T. Funke, R. S. Selzer, A. Levinstone, *FACTANAL, Program 320*, Quantum Chemistry Echange, Indiana University, Bloomington, Ind., 1976.

3. Arendale, W. F. and Jeffreys, Harold B., *Study of Reflected Energy From Laser Illuminated Targets*, Final Report Contract DA-01-021-AMC-12250(z). Also issued as UARI Research Report No. 58, December 1968 (not in print). Harold B. Jefferys, *The Reflection of Polarized Light From Near Diffused Surfaces* M.S. Thesis is available from the University of Alabama Library, Tuscaloosa, Alabama.

4. Hecht, Harry G., "A comparison of the Kubelka-Munk, Rozenberg, and Pitts-Giovanelly Methods of Analysis of Diffuse Reflectance for Several Model Systems", *Applied Spectroscopy* 1983, *37*, 348.